CSIRO PUBLISHING

International Journal of Wildland Fire **2010**, *19*, 346–363 www.publish.csiro.au/journals/ijwf

Turbulent kinetic energy during wildfires in the north central and north-eastern US

Warren E. Heilman[A,B] *and Xindi Bian*[A]

[A]Northern Research Station, USDA Forest Service, East Lansing, MI 48823, USA.
[B]Corresponding author. Email: wheilman@fs.fed.us

Abstract. The suite of operational fire-weather indices available for assessing the atmospheric potential for extreme fire behaviour typically does not include indices that account for atmospheric boundary-layer turbulence or wind gustiness that can increase the erratic behaviour of fires. As a first step in testing the feasibility of using a quantitative measure of turbulence as a stand-alone fire-weather index or as a component of a fire-weather index, simulations of the spatial and temporal patterns of turbulent kinetic energy during major recent wildfire events in the western Great Lakes and north-eastern US regions were performed. Simulation results indicate that the larger wildfires in these regions of the US were associated with episodes of significant boundary-layer ambient turbulence. Case studies of the largest recent wildfires to occur in these regions indicate that the periods of most rapid fire growth were generally coincident with occurrences of the product of the Haines Index and near-surface turbulent kinetic energy exceeding a value of $15\,m^2\,s^{-2}$, a threshold indicative of a highly turbulent boundary layer beneath unstable and dry atmospheric layers, which is a condition that can be conducive to erratic fire behaviour.

Introduction

Daily 24–72-h fire-weather predictions for different regions of the US are now readily available from the regional Fire Consortia for Advanced Modelling of Meteorology and Smoke (FCAMMS) (http://fcamms.org, accessed 12 March 2010) that were established as part of the US National Fire Plan (USDA Forest Service 2002). These predictions are based on daily simulations of atmospheric conditions and fire-weather indices over specific modelling domains using the fifth generation Penn State University (PSU)–National Center for Atmospheric Research (NCAR) mesoscale model (MM5) (Grell *et al*. 1994). The MM5 has been evaluated and used extensively for research and operational weather and air-quality forecasting activities in the US and internationally since its development (e.g. Manning and Davis 1997; Reisner *et al*. 1998; Colle *et al*. 1999, 2000, 2003*a*, 2003*b*; de Arellano *et al*. 2001; Chien *et al*. 2002; Zhong and Fast 2003; Zhong *et al*. 2005; Byun and Schere 2006). Included in the suite of fire-weather indices provided by the FCAMMS are many operational-type indices that are calculated based solely on the non-turbulent state of the atmosphere (e.g. Haines Index (HI) (Haines 1988), Ventilation Index (VI) (Ferguson *et al*. 2001), Fosberg Index (FI) (Fosberg 1978)). However, atmospheric turbulence (e.g. wind gustiness) can also influence the behaviour of fires and the transport and diffusion of heat, moisture and gases in fire environments. With the development and application of new state-of-the-art atmospheric mesoscale, boundary-layer and coupled fire–atmosphere models and the deployment of sophisticated instrumentation for monitoring turbulence regimes within and in the vicinity of actual burn events, it is now possible to begin examining the role of ambient atmospheric turbulence and its interaction with fire-induced turbulence in affecting fire behaviour. For example, previous modelling studies such as Heilman (1994), Linn *et al*. (2002, 2005, 2007), Linn and Cunningham (2005), Mell *et al*. (2007), Cunningham *et al*. (2005), Coen (2005), Clark *et al*. (2004), Jenkins (2002) and Sun *et al*. (2006) have shown the importance of small-scale atmospheric processes at spatial and temporal scales relevant to atmospheric turbulence in affecting local fire behaviour and fire–atmosphere interactions. The recent observational studies of Clark *et al*. (1999), Coen *et al*. (2004) and Clements *et al*. (2006, 2007, 2008) have also provided valuable insight into the turbulence regimes that exist in fire environments.

One particular turbulence variable or index that has been studied extensively in the context of fundamental boundary-layer dynamics, and to a lesser extent in the context of wildland fires, is turbulent kinetic energy (TKE) (Mellor and Yamada 1974). Turbulent kinetic energy is defined as the kinetic energy per unit mass associated with eddies in turbulent flow. The generation and dissipation of TKE are dependent on the amount of ambient wind shear present and the stability (buoyancy) within an atmospheric layer. Although previous modelling and observational studies have provided valuable insight into TKE production, dissipation, transport and evolution under different surface and mean atmospheric conditions, the efficacy of TKE as an indicator or predictor of how conducive the atmospheric boundary layer will be to extreme or erratic fire behaviour has not been tested. The availability of predictions of TKE from the FCAMMS MM5-based fire-weather simulations, using level 2.5 of the Mellor–Yamada turbulence hierarchy (Mellor and Yamada 1974, 1982; Gerrity *et al*. 1994), provides an opportunity to examine the prevalence of significant ambient boundary-layer turbulence during major wildland fire events and the feasibility of using TKE in some fashion as an atmospheric indicator of potential erratic fire behaviour.

10.1071/WF08076 1049-8001/10/030346

This paper is a first step in examining the utility of using boundary-layer turbulence, as measured by TKE, for assessing the atmospheric potential for extreme or erratic fire behaviour. Output from the FCAMMS–Eastern Area Modelling Consortium (EAMC) MM5 fire-weather predictions is used to examine the temporal and spatial evolution of TKE during previous wildfire events in the north central and north-eastern US and the relative significance of boundary-layer turbulence in contributing to wildfires of different sizes in these regions.

Turbulent kinetic energy description

While atmospheric conditions and variables such as stability, mean wind speeds and moisture concentrations in atmospheric layers within and above the boundary layer can influence fire behaviour, turbulent atmospheric circulations (i.e. wind gusts) within the boundary layer can also create an environment conducive to erratic fire behaviour. Wind gusts are manifestations of turbulent eddies generated by wind shear and buoyancy effects, which can be very large in the boundary layer. The amount of energy in these turbulent eddies is defined as TKE, and is given by $0.5q^2$ where

$$q^2 = \overline{u'^2} + \overline{v'^2} + \overline{w'^2} \quad (1)$$

and $\overline{u'^2}$, $\overline{v'^2}$ and $\overline{w'^2}$ are the variances of the perturbation (turbulent) velocities in the horizontal x, horizontal y and vertical z directions respectively. Large vertical wind shears under thermally unstable (convective) conditions lead to a highly energetic turbulence regime (i.e. large TKE values), whereas a thermally stable environment will tend to suppress any turbulence generated by mechanical wind shears and produce more laminar-type flows (low TKE values). Irrespective of the enhanced atmospheric turbulence generated by buoyancy and wind shears associated with a fire, an already highly turbulent atmospheric boundary layer can contribute to even more erratic fire behaviour through interactions between the fire-induced and ambient boundary-layer turbulence regimes.

Simulations and predictions of TKE are possible in many of the current research and operational atmospheric mesoscale and boundary layer numerical models, including MM5. Turbulent kinetic energy can be simulated and predicted using the level-2.5 closure scheme from Mellor and Yamada (1974, 1982) given by

$$\frac{\partial}{\partial t}\left(\frac{q^2}{2}\right) + V \cdot \nabla \frac{q^2}{2} - \frac{\partial}{\partial z}\left[K_q \frac{\partial}{\partial z}\left(\frac{q^2}{2}\right)\right] = P_s + P_b - \varepsilon \quad (2)$$

where the terms on the left side of the equation represent the local-time rate of change of TKE, the advection of TKE by the three-dimensional mean wind V and the vertical diffusion of TKE (parameterised in terms of diffusion coefficient K_q). The terms on the right side of the equation represent the production of TKE through vertical wind shear effects (P_s), the production or dissipation of TKE through buoyancy effects (P_b) and the non-buoyant dissipation of TKE (ε) via the breakdown of turbulent eddies into smaller and smaller sizes. The production (P_s) of TKE through vertical wind shear effects is given by

$$P_s = -\overline{u'w'}\frac{\partial \overline{u}}{\partial z} - \overline{v'w'}\frac{\partial \overline{v}}{\partial z} \quad (3)$$

and the buoyant production or dissipation (P_b) of TKE is given by

$$P_b = \frac{g}{\theta_v}\overline{\theta'_v w'} \quad (4)$$

where g is the acceleration due to gravity, $\overline{u}$ and $\overline{v}$ are the horizontal components of the mean wind, θ_v is the virtual potential temperature, and $\overline{u'w'}$, $\overline{v'w'}$ and $\overline{\theta'_v w'}$ are the vertical turbulent fluxes of momentum and heat. The MM5 mesoscale model used in this study includes the Mellor and Yamada (1974, 1982) TKE formulation and is described in more detail by Gerrity *et al.* (1994).

Unlike other fire-weather indices such as the HI, FI and VI, which can all be easily computed from surface or radiosonde observations or from numerical model output, TKE as a potential fire-weather index has not been used extensively because it is fairly complex and is rarely, if ever, included in the suite of fire-weather variables made available to fire managers. However, the increasing availability and delivery of TKE predictions from research and development groups like the FCAMMS have now made it possible to assess the significance of ambient atmospheric turbulence before, at the onset of and during wildland fires. It is through this assessment that the effective use of TKE alone or in combination with other fire-weather indices as an additional atmospheric indicator of potential erratic fire behaviour can be tested.

Methods

Study area

Daily fire-weather predictions from the EAMC MM5 simulations incorporate four spatial domains covering the continental US, the eastern US, the western Great Lakes region and the New England states, with corresponding MM5 horizontal grid-point spacings of 36, 12, 4 and 4 km respectively (Fig. 1). For this study of atmospheric TKE during wildland fires, the spatial domains covering the western Great Lakes region and the New England states were chosen to take advantage of the higher-resolution MM5 output data available in these areas. The western Great Lakes region includes the states of Minnesota, Wisconsin, Michigan and the northern portions of Iowa, Illinois, Indiana and Ohio. The New England region includes all the states from the southern half of Maine south-westward to the northern portions of Virginia and West Virginia.

Fire occurrence data

Wildland fire data for the period of 1 January 2005–31 May 2007 were obtained from the Geospatial Multi-Agency Coordination (GeoMAC) internet-based mapping tool for displaying current and past wildfire locations and ancillary data associated with each fire (http://geomac.usgs.gov/, accessed 11 March 2010). Fire names, fire locations (state, latitude and longitude), fire start and end dates and total acres burned were recorded for all reported wildland fires in GeoMAC that burned 0.4047 km^2 (100 acres) or more within the previously defined western Great Lakes and New England spatial domains. A total of 104 wildfires were noted that met these fire size and fire location criteria. Tables 1 and 2 provide a listing of the wildfires used in this study, grouped by fires that burned 4.047 km^2 (1000 acres) or more (hereafter referred to as large fires) and fires that burned

Table 1. Turbulent kinetic energy at the surface (TKE_s), Haines Index (HI), the product of the HI and TKE_s, Richardson number at the surface (Ri_s), and the mixing height (MH) at the location and date and time of maximum HI × TKE_s for wildfires that burned 4.047 km^2 (1000 acres) or more in the north central and north-eastern US from 1 January 2005 to 31 May 2007

Fire sizes in brackets are in acres. Values of HI × TKE_s exceeding 15 m^2 s^{-2} are shown in bold

Fire name	State	Start date	Contained date	Size (km^2)	TKE_s (m^2 s^{-2})	HI	HI × TKE_s (m^2 s^{-2})	Ri_s	MH (m)
Ham Lake	MN[A]	05-May-07	19-May-07	307.0 [75 851]	6.421	6	**38.527**	−0.047	1192
Cavity Lake	MN	14-Jul-06	01-Sep-06	128.8 [31 830]	5.366	6	**32.198**	−0.314	1549
Warren Grove	NJ	15-May-07	21-May-07	69.9 [17 270]	3.983	4	**15.933**	−0.142	628
Peatland	MN	06-Oct-06	08-Oct-06	26.8 [6625]	8.197	2	**16.394**	−0.013	918
SUF-East Zone Comp.	MN	08-Sep-06	01-Oct-06	23.9 [5898]	3.770	6	**22.622**	−0.028	1499
Hughes Lake	MI	30-Apr-06	05-May-06	23.5 [5817]	3.691	4	14.765	−0.082	2351
Reiner	MN	28-Apr-07	29-May-07	21.7 [5350]	2.661	5	13.304	−0.052	2585
Red Lake 05	MN	12-Apr-07	13-Apr-07	20.9 [5157]	1.462	4	5.846	−0.090	367
Red Lake 16	MN	06-Apr-06	07-Apr-06	14.8 [3650]	4.535	4	**18.139**	−0.053	447
Carroll/Hamre	MN	28-Apr-07	30-Apr-07	14.3 [3536]	2.540	5	12.701	−0.053	2583
Cottonville	WI	05-May-05	06-May-05	13.8 [3410]	3.128	3	9.383	−0.116	2950
Border	MN	03-May-07	07-May-07	12.5 [3099]	4.739	5	**23.697**	−0.044	608
Guinea Marsh	MD	10-Feb-07	13-Feb-07	10.3 [2537]	2.905	5	14.527	−0.185	576
Deerwood	MN	14-Apr-07	N/A	10.1 [2500]	0.413	5	2.065	−99.000	225
Deano/Benville	MN	29-Apr-07	29-Apr-07	9.6 [2377]	3.129	4	12.516	−0.153	949
Red Lake 181	MN	14-Apr-05	15-Apr-05	8.9 [2210]	2.781	5	13.904	−0.122	1166
Jupiter	MN	20-Apr-07	N/A	8.9 [2200]	3.132	5	**15.66**	−0.217	1780
Turtle Lake	MN	13-Jul-06	N/A	8.4 [2085]	1.423	4	5.690	−0.410	636
Beaches Lake	MN	20-Apr-07	20-Apr-07	8.1 [2000]	3.174	5	**15.869**	−0.187	1780
McKinley	MN	12-Apr-06	13-Apr-07	8.1 [2000]	2.351	4	9.403	−0.530	588
Cardinal	VA	30-Apr-06	07-May-06	7.8 [1935]	4.655	3	13.965	−0.148	952
Red Lake 45	MN	05-Apr-05	06-Apr-05	6.6 [1620]	1.958	3	5.873	−0.038	473
Halma	MN	20-Apr-07	20-Apr-07	6.5 [1600]	3.299	5	**16.497**	−0.281	1799
Savanna Lake Complex	MD	03-Mar-05	04-Mar-05	6.4 [1578]	0.813	4	3.254	−0.113	715
Bear Trap	PA	05-May-06	08-May-06	6.2 [1531]	2.011	5	10.055	−0.402	940
Grain Bin	MN	26-Apr-06	27-Apr-06	6.1 [1496]	2.519	4	10.077	−0.280	1182
20 Mile	MN	26-Apr-06	27-Apr-06	5.9 [1456]	2.519	4	10.077	−0.280	1182
Beckers Island	MD	26-Jan-06	28-Jan-06	5.7 [1400]	4.812	4	**19.249**	−0.251	913
Alpine Lake	MN	06-Aug-05	19-Aug-05	5.4 [1335]	3.729	6	**22.377**	−0.118	501
Island Creek	MD	17-Jan-05	17-Jan-05	5.3 [1300]	1.106	5	5.532	−0.079	714
Barrel	MN	11-Apr-07	N/A	5.2 [1280]	3.817	3	11.451	−0.080	578
Pioneer	WI	29-Apr-07	01-May-07	4.7 [1167]	3.149	6	**18.894**	−0.024	619
Five Mile	PA	10-May-06	11-May-06	4.2 [1042]	2.939	3	8.818	−0.025	482
River Road	MN	17-Apr-07	N/A	4.0 [1000]	0.587	4	2.349	−51.638	934
Bartz	MN	28-Apr-07	N/A	4.0 [1000]	2.902	5	14.51	−0.046	2584
Mean					3.160	4.429	13.889	−4.447	1148
Median					3.128	4	13.904	−0.118	934

[A]Ham Lake fire also burned into Ontario, Canada.

less than 4.047 km^2 (1000 acres) (hereafter referred to as small fires) respectively.

The fire occurrence data compiled for this study were limited in that most of the data did not include observed incremental rate of growth information, which can be used as a potential indicator of extreme or erratic fire behaviour. The use of the terms 'extreme' or 'erratic' in characterising fire behaviour typically implies very high rates of fire spread, significant crowning (assuming the presence of overstorey vegetation) and significant spotting. These fire properties may lead to larger burn areas and they are all influenced by atmospheric turbulence regimes that, to a large extent, govern the thermal and dynamic environments surrounding wildfires. As incremental fire data for most of the fires included in Tables 1 and 2 were not available, final fire size was used as the basis for the initial statistical analyses carried out in this study (*Results and discussion* section) to assess the relative importance of ambient atmospheric turbulence in affecting the behaviour of past fires in the north central and north-eastern US.

MM5 fire-weather simulations

For each wildfire event, gridded MM5 output data and post-processed fire-weather index data from the appropriate modelling domain and covering the duration of the event were extracted from the EAMC MM5 fire-weather prediction archive, including TKE, HI, mixing height, temperature, dew-point temperature, wind speed and wind direction data. Output data for 6–12 h before the onset of each fire were also extracted from the

Table 2. Turbulent kinetic energy at the surface (TKE_s), Haines Index (HI), the product of the HI and TKE_s, Richardson number at the surface (Ri_s), and the mixing height (MH) at the location and date and time of maximum HI × TKE_s for wildfires that burned between 0.405 km^2 (100 acres) and 4.047 km^2 (1000 acres) in the north central and north-eastern US from 1 January 2005 to 31 May 2007

Fire sizes in brackets are in acres. Values of HI × TKE_s exceeding 15 $m^2 s^{-2}$ are shown in bold

Fire name	State	Start date	Contained date	Size (km^2)	TKE_s ($m^2 s^{-2}$)	HI	HI × TKE_s ($m^2 s^{-2}$)	Ri_s	MH (m)
Cherrytown	NY	30-Apr-06	09-May-06	3.8 [933]	4.810	5	**24.048**	−0.103	944
Range	MA	16-Apr-05	N/A	3.2 [800]	1.498	5	7.491	−0.206	1192
Cederbend WMA	MN	21-Nov-06	22-Nov-06	2.9 [727]	0.908	5	4.538	1.048	294
Twistol Swamp	MN	23-Apr-07	23-Apr-07	2.8 [680]	1.840	4	7.358	−23.540	741
Trail	MN	10-Apr-06	11-Apr-06	2.7 [676]	2.795	4	11.178	−0.049	479
Delta	MA	29-Apr-06	30-Apr-06	2.6 [650]	2.509	5	12.543	−0.928	1155
Richardville	MN	22-Apr-06	N/A	2.6 [640]	1.191	4	4.764	−1.388	959
Pitt	MN	28-Apr-07	29-Apr-07	2.5 [630]	2.763	5	13.815	−0.199	763
Mosquito Ditch	MD	03-Mar-05	03-Mar-05	2.5 [618]	1.422	4	5.688	−0.525	889
Como 2	MN	24-Apr-05	N/A	2.4 [600]	2.325	3	6.974	−0.140	296
PA-PAS-042026	PA	01-Oct-05	06-Oct-05	2.4 [600]	1.572	5	7.862	−0.078	1201
Swimming Gut	MD	26-Jan-06	28-Jan-06	2.4 [600]	0.989	4	3.956	−0.577	913
Foxboro	WI	29-Apr-07	30-Apr-07	2.4 [590]	5.690	4	**22.760**	−0.081	1491
Red Lake 197	MN	16-Apr-06	16-Apr-06	2.2 [550]	1.765	5	8.824	−0.161	486
Star	MN	25-Apr-07	25-Apr-07	2.2 [550]	1.354	3	4.063	−1.967	1175
Centerville	ME	09-May-06	11-May-06	2.2 [550]	2.824	5	14.118	−0.158	1187
Grays Island	MD	28-Jan-06	28-Jan-06	2.1 [518]	0.417	5	2.087	−1.201	228
Black River	MN	16-Apr-06	N/A	2.0 [500]	1.739	5	8.696	−0.049	615
Mississippi Meadows	MN	05-May-05	07-May-05	1.9 [475]	5.352	5	**26.758**	−0.080	762
Raritan Center	NJ	27-Jan-06	27-Jan-06	1.9 [465]	1.688	4	6.753	−0.207	736
Curry Range	MA	21-Apr-07	23-Apr-07	1.8 [450]	3.436	5	17.181	−0.078	1503
Thorofare 1	MD	09-Jan-06	09-Jan-06	1.8 [439]	3.900	4	15.601	0.003	606
Vikings Kicker	MN	06-May-05	N/A	1.7 [432]	1.543	3	4.630	−0.493	941
Lick Run	PA	03-May-06	05-May-06	1.7 [424]	3.115	4	12.460	−0.306	1803
Thorofare 2	MD	16-Jan-07	17-Jan-07	1.7 [411]	3.167	5	**15.837**	−0.099	1735
Frozen Ground	MN	03-Apr-05	N/A	1.6 [400]	0.589	4	2.357	−1.154	743
Wake-up	MN	24-Apr-07	N/A	1.6 [400]	1.270	3	3.810	−45.075	935
Rice Lake 2	MI	08-Aug-05	N/A	1.6 [389]	0.200	4	0.800	−0.154	10
Pound Marsh	MD	16-Feb-06	16-Feb-06	1.5 [371]	0.241	4	0.966	0.660	129
Bull Point	MD	10-Feb-07	11-Feb-07	1.5 [370]	3.281	4	13.124	−0.193	1110
Sandy Ridge	PA	30-Mar-06	31-Mar-06	1.4 [352]	3.802	3	11.407	−76.598	1185
Indiantown Gap	PA	29-Apr-06	30-Apr-06	1.4 [350]	1.783	4	7.131	−0.354	745
Easter Sunday	MN	16-Apr-06	N/A	1.4 [348]	1.396	6	8.376	−0.383	1476
Pokata Creek II	MD	15-Feb-06	16-Feb-06	1.4 [345]	0.615	4	2.458	1.053	176
Treaster Kettle	PA	01-May-06	04-May-06	1.4 [340]	2.446	5	12.229	−0.187	756
Parkers Prairie	MN	09-Apr-06	11-Apr-06	1.3 [326]	2.795	4	11.178	−0.049	602
Red Lake 245	MN	18-Apr-05	19-Apr-05	1.3 [320]	2.839	4	11.355	−0.207	751
Casebeer Lake	MN	08-Apr-05	08-Apr-05	1.3 [320]	5.029	5	**25.144**	−99.000	949
B Loop	DC	27-Mar-07	29-Mar-06	1.3 [318]	2.699	5	13.495	−0.994	929
Sharptail Burn	MN	17-Apr-06	N/A	1.3 [317]	3.222	5	16.108	−0.280	946
Norris Road	MN	27-Mar-07	N/A	1.2 [304]	2.323	2	4.646	−0.015	592
Savanna Lake	MD	01-Feb-06	01-Feb-06	1.2 [300]	0.200	4	0.800	−99.000	10
Green Mountain	PA	11-May-05	13-May-05	1.0 [256]	3.876	5	**19.380**	−0.350	470
Blue Lake	MI	11-Apr-05	11-Apr-05	1.0 [250]	3.744	5	**18.718**	−0.034	367
219	MN	19-Jul-06	24-Jul-06	1.0 [240]	2.667	4	10.668	−0.345	1534
Lewis Peak	VA	01-May-07	04-May-07	0.9 [215]	5.449	4	**21.797**	−0.046	1515
Hound	MN	03-Apr-05	03-Apr-05	0.8 [200]	0.556	5	2.779	−99.000	593
Gillman	MN	04-May-05	N/A	0.8 [200]	2.157	3	6.472	−0.744	1443
Shack	MN	06-Apr-06	N/A	0.8 [200]	2.908	3	8.723	−0.020	292
Shannondale	WV	26-Nov-05	30-Nov-05	0.8 [200]	5.272	3	**15.817**	−0.014	965
Correction Corner	MN	13-May-07	18-May-07	0.7 [182]	3.496	5	**17.480**	−0.205	1780
Ramsey	MN	09-Apr-05	09-Apr-05	0.7 [166]	2.583	5	12.915	−0.122	604
King Shoals	WV	13-Mar-07	N/A	0.7 [162]	2.479	2	4.959	−0.098	1479
Unnamed	MI	30-Apr-05	30-Apr-05	0.6 [158]	2.483	3	7.449	−1.220	473
Section 32	MN	13-May-07	14-May-07	0.6 [150]	2.798	4	11.191	−0.298	986
South Boundary 262	MN	09-May-07	11-May-07	0.6 [150]	3.109	5	**15.546**	−1.164	603

(*Continued*)

Table 2. (Continued)

Fire name	State	Start date	Contained date	Size (km^2)	TKE$_s$ (m^2 s^{-2})	HI	HI × TKE$_s$ (m^2 s^{-2})	Ri_s	MH (m)
Cherry	MN	10-May-07	15-May-07	0.6 [150]	3.589	5	**17.944**	−0.934	613
Camber	VA	19-Mar-05	21-Mar-05	0.6 [150]	6.897	5	**34.487**	−0.001	166
Clementson	MN	04-Sep-06	12-Sep-06	0.6 [149]	2.923	6	**17.537**	−0.167	980
Emmons Complex	WI	13-Apr-05	13-Apr-05	0.6 [142]	2.107	4	8.429	−0.203	596
Sunrise Lake	NJ	22-Mar-06	22-Mar-06	0.6 [139]	4.588	4	**18.354**	−0.052	1412
Happy Acres	PA	07-May-07	07-May-07	0.5 [135]	1.352	4	5.409	−2.528	753
Crawford	VA	27-Mar-07	28-Mar-07	0.5 [115]	2.955	5	14.775	−0.047	616
Douglas Center 2	IN	06-May-05	06-May-05	0.5 [112]	3.351	3	10.052	−5.689	1188
Bald Eagle	PA	20-Apr-06	20-Apr-06	0.4 [110]	0.911	5	4.555	−1.445	965
Keystone	MI	03-Aug-06	05-Aug-06	0.4 [106]	0.516	5	2.578	−0.030	635
Wobble Grade	MN	12-Jul-06	N/A	0.4 [100]	1.418	5	7.088	−2.992	645
Famine	MN	08-Sep-06	01-Oct-06	0.4 [100]	3.282	5	**16.411**	−18.043	489
Merrick Spring	PA	06-May-05	07-May-05	0.4 [100]	2.435	4	9.738	−2.764	1160
Mean					2.540	4.290	10.965	−7.131	847
Median					2.509	4	10.052	−0.206	762

archive to capture the ambient atmospheric conditions before each ignition. The EAMC MM5 archive consists of hourly gridded MM5 model output data from daily, 48-h simulations initialised with 0000 hours (all times are shown in Coordinated Universal Time, UTC) output data from the US National Oceanic and Atmospheric Administration's (NOAA) 40-km grid-spacing North American Mesoscale (NAM) Model run by the National Centers for Environmental Prediction (NCEP).

Following the methodology of Heilman and Bian (2007), the extracted EAMC MM5 fire-weather simulation data were used to compute the product of the HI and near-surface (∼10 m above ground level) TKE (HI × TKE$_s$) at every hour for the duration of each of the 104 wildfire events considered in this study. The HI is a measure of the instability and dryness of lower to middle tropospheric layers. Haines (1988) noted that dry and unstable air increases the probability that wildland fires with significant convective plumes (i.e. plume-dominated fires) will become large and erratic. He devised an atmospheric mesoscale type index that characterises both the stability and moisture content of specific atmospheric layers, depending on the elevation above sea level of the underlying terrain. Although the HI is frequently applied as an operational fire-weather index only when mean wind speeds in the atmospheric layers below the layer where the HI is calculated are relatively low, the 104 wildfire events considered in this study were not filtered according to mean wind speeds. Atmospheric turbulence in the lower atmosphere, whether generated primarily by strong mean wind shears or primarily through buoyancy effects, enhances the mixing of air between atmospheric layers. This enhanced mixing of the ambient air, in addition to the vertical mixing associated with convective plumes from any wildland fires that may be present, may increase the likelihood of dry, unstable and possibly high-momentum air from aloft (large HI values) mixing down to the surface and contributing to extreme or erratic fire behaviour. Combining the HI and TKE$_s$ via a simple product of the two produces a highly discriminatory index that captures those relatively rare events when both the atmospheric mesoscale environment, as quantified by the HI, and the atmospheric boundary-layer environment, as quantified by near-surface TKE, may lead to extreme and erratic fire behaviour.

For each wildfire event, maximum values of HI × TKE$_s$ and the dates and times of their occurrence were determined. At the date and time of each occurrence of maximum HI × TKE$_s$ values, the HI, TKE$_s$, surface (∼2 m above ground level) Richardson number (Ri_s), mixing height, average TKE in the mixed layer and profiles of TKE and Richardson number were noted or calculated from the MM5 wind, temperature and moisture output data. Analysis of these variables provides insight into the ambient atmospheric boundary-layer turbulence regimes that can influence fire behaviour at the same time the atmospheric mesoscale environment is conducive to extreme fire behaviour, the physical mechanisms most often responsible for the generation of significant boundary-layer turbulence during major wildfire events in the north central and north-eastern US, and the characteristic spatial and temporal evolution of ambient boundary-layer turbulence during wildfire events in these regions.

Results and discussion

Summary statistics

Summary statistics for the 104 wildfires included in this study, ordered by the area burned, are shown in Tables 1 and 2. There were 35 reported large wildfires in the western Great Lakes region and New England region during the period 1 January 2005 to 31 May 2007 (Table 1) and 69 reported small wildfires (Table 2). For the 35 large wildfire events, 13 of them (37.1%) had maximum values of HI × TKE$_s$ exceeding 15 m^2 s^{-2}. This threshold generally corresponds to an HI ≥ 5 and TKE$_s$ ≥ 3 m^2 s^{-2} and is indicative of a highly turbulent boundary layer beneath unstable and dry atmospheric layers, a condition that can be conducive to erratic fire behaviour (Heilman and Bian 2007). The five largest wildfires all had periods when maximum HI × TKE$_s$ values exceeded 15 m^2 s^{-2}, even though HI values at the time of maximum HI × TKE$_s$ for two of the wildfires (Warren Grove Fire, NJ; Peatland Fire, MN) were less than 5. The average (median) maximum HI × TKE$_s$ value for the 35 large wildfires was 13.889 m^2 s^{-2} (13.904 m^2 s^{-2}), just slightly less than the specified threshold for an atmospheric environment highly conducive to erratic fire behaviour.

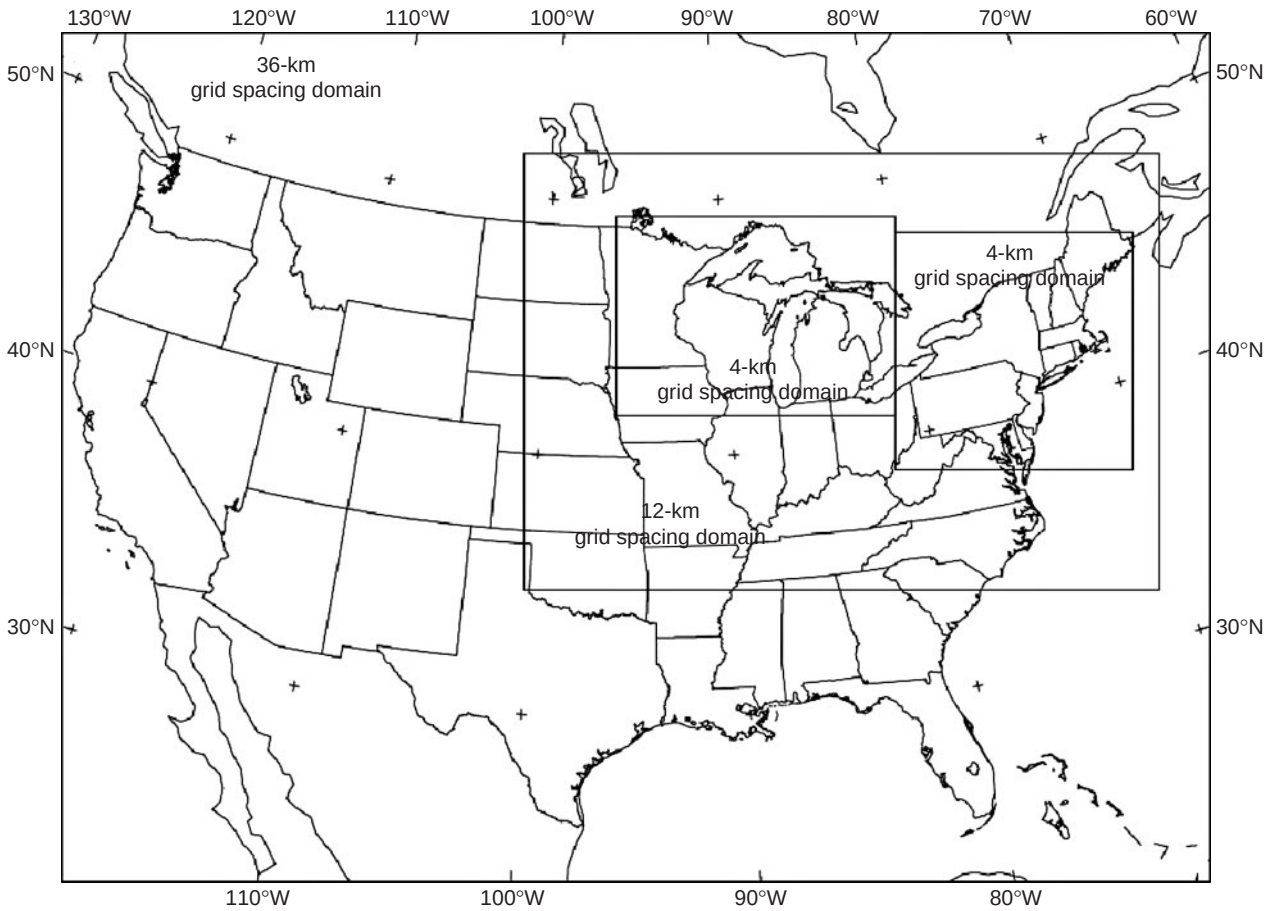

Fig. 1. MM5 spatial domains used by the Eastern Area Modelling Consortium for fire-weather predictions over the United States.

Near-surface TKE values (TKE_s) averaged $3.160\,m^2\,s^{-2}$ (median $= 3.128\,m^2\,s^{-2}$) at the time of maximum HI $\times$ TKE_s for the large wildfires (Table 1), with TKE_s exceeding $6\,m^2\,s^{-2}$ during the May 2007 Ham Lake and the October 2006 Peatland fires in Minnesota. These extremely high TKE values near the surface indicate substantial wind gusts and highly variable wind regimes were present that likely contributed to the overall behaviour of these fires. More than half (18) of the large wildfires had periods of TKE_s exceeding $3\,m^2\,s^{-2}$ and six out of the eight wildfires that burned more than $20.234\,km^2$ (5000 acres) had periods of TKE_s exceeding $3\,m^2\,s^{-2}$. The duration of the periods when TKE_s exceeded $3\,m^2\,s^{-2}$ was highly variable during each wildfire event and between wildfire events. For example, during the Ham Lake wildfire, periods when TKE_s values exceeded the $3\,m^2\,s^{-2}$ threshold ranged from 1 to 49 h. For the entire Ham Lake wildfire event (reported start date: 5 May 2007; reported containment date: 19 May 2007), TKE_s values exceeded the $3\,m^2\,s^{-2}$ threshold nearly 26% of the time. This is in contrast to other large wildfire events such as the Superior National Forest (SUF) East Zone Complex fire in Minnesota (reported start date: 8 September 2006; reported containment date: 1 October 2006). Periods when the 3-$m^2\,s^{-2}$ TKE_s threshold was exceeded ranged in duration from 1 to 22 h for this wildfire, with TKE_s values exceeding the 3-$m^2\,s^{-2}$ threshold less than 9% of the time for the entire event. In comparison, the analysis of TKE_s values over the western Great Lakes region for all days in 2006 conducted by Heilman and Bian (2007) suggests that mid-afternoon (2000 hours UTC) TKE_s values typically exceed the 3-$m^2\,s^{-2}$ threshold approximately once every 10 days at any particular location within this domain (Fig. 1). More comprehensive analyses of the long-term climatological patterns of hourly TKE_s values over the north central and north-eastern US are required in order to fully assess how the frequency of occurrence and duration of high TKE_s values during and at the location of wildfire events compares with the climatological average frequency and duration of high TKE_s values at those same locations.

For the 69 small wildfires (Table 2), only 16 of them (23.2%) had maximum HI $\times$ TKE_s values that exceeded $15\,m^2\,s^{-2}$. The mean maximum HI $\times$ TKE_s value for these smaller wildfires was $10.965\,m^2\,s^{-2}$ (median $= 10.052\,m^2\,s^{-2}$) whereas the mean TKE_s value at the time of maximum HI $\times$ TKE_s was $2.540\,m^2\,s^{-2}$ (median $= 2.509\,m^2\,s^{-2}$). Applying Student's *t*-test in this case, with the TKE_s distributions for the small and large wildfire groups satisfying the normality ($P > 0.050$) and equal variance ($P = 0.943$) requirements, the difference in mean TKE_s values at the time of maximum HI $\times$ TKE_s between the large and small wildfire groups was found to be statistically significant ($t = 1.992$, $P = 0.049$). Although there is a statistically

significant difference in mean TKE_s values between the two groups of wildfires, the difference in median HI values at the time of maximum HI × TKE_s between the two groups is not statistically significant (Mann–Whitney rank sum test: $P = 0.554$). Here, the Mann–Whitney rank sum test was applied because of the discrete value characteristic of the HI and the non-normal HI distributions ($P < 0.001$) for the small and large wildfire groups. These results suggest that when the atmospheric mesoscale and boundary-layer environments are collectively conducive to erratic or extreme fire behaviour in the north central and north-eastern US (as quantified in this case by the product of the HI and TKE_s), TKE_s may be a better discriminating atmospheric indicator than the categorically based HI of whether a wildfire, if present, has the potential to become erratic and large.

The difference in mean mixing height values (1148 *v.* 847 m) at the time of maximum HI × TKE_s between the two groupings of wildfires in Tables 1 and 2 reveals that large wildfires in the north central and north-eastern US are more likely to have higher mixing heights at the time of maximum HI × TKE_s than small wildfires, although the difference in median mixing height values between the two groups (933.9 *v.* 761.6 m) was not statistically significant (Mann–Whitney rank sum test: $P = 0.196$). Here again, the Mann–Whitney rank sum test was applied because the mixing height distributions were found to be non-normal ($P < 0.001$). The mean and median mixing height differences between the two groupings are qualitatively consistent with the statistically significant difference in mean TKE_s values between the two groups in that substantial turbulence in the boundary layer can increase overall mixing heights.

The spatial and temporal patterns of atmospheric turbulence observed in the boundary layer are the direct result of wind shear and buoyancy conditions that govern the generation and dissipation of turbulent eddies. The relative significance of wind shear *v.* buoyancy in contributing to ambient turbulence regimes during wildfires can be assessed via a simple *Ri* analysis, with *Ri* given by

$$Ri = \frac{g}{\theta} \frac{\partial\theta/\partial z}{((\partial U/\partial z)^2 + (\partial V/\partial z)^2)} \quad (5)$$

where θ is the potential temperature, and U and V are the east–west and north–south ambient wind components respectively. Negative values of *Ri* less than −0.03 indicate the generation of turbulence is dominated by buoyancy effects, whereas negative values greater than −0.03 indicate wind shears are the primary mechanism in generating turbulence. Positive values of *Ri* between 0 and 0.25 indicate the mechanical generation of turbulence in a thermally stable environment. Richardson numbers greater than 0.25 indicate the presence of a sufficiently stable thermal environment to dissipate any turbulence generated by mechanical wind shears.

Included in Tables 1 and 2 are computed near-surface *Ri* values (Ri_s) at the time of maximum HI × TKE_s for each wildfire event. For the 35 large wildfires, 31 had Ri_s values at the time of maximum HI × TKE_s that were less than −0.03 (Table 1). Similarly, for the 69 small wildfires, 61 had Ri_s values less than −0.03 at the time of maximum HI × TKE_s (Table 2). The computed Ri_s values clearly show that ambient buoyancy was the overriding factor in generating the ambient near-surface turbulence at the time of maximum HI × TKE_s for the wildfire events considered in this study. However, the larger mean Ri_s (−4.447) and median Ri_s (−0.118) associated with the large wildfires (Table 1) compared with the mean Ri_s (−7.131) and median Ri_s (−0.206) associated with the small wildfires (Table 2) suggest that turbulence generation by mechanical wind shear was more prominent during the large wildfire events, though often not enough to dominate the buoyancy effects.

Individual case studies

The three most significant wildfires to occur in the north central and north-eastern US during the 2005–07 period were the Ham Lake and Cavity Lake fires in northern Minnesota and the Warren Grove fire in New Jersey (Table 1). Each of these wildfires had periods when the product of the HI and TKE_s exceeded 15 $m^2 s^{-2}$, the threshold for a highly turbulent boundary-layer beneath a dry and unstable atmospheric layer. The spatial and temporal patterns of the ambient boundary-layer turbulence regimes during these particular fires were examined in relation to the reported cumulative area burned during the fires and the mechanisms involved in generating the turbulence.

The Ham Lake fire burned 307.0 km^2 (75 851 acres) in the Boundary Waters Canoe Area Wilderness in north-eastern Minnesota and southern Ontario (48°5′56.40″N, −90°50′52.80″W) during the period 5 to 19 May 2007. The boreal forest mixture of hardwoods and conifers in this area experienced a major derecho (straight-line windstorm) on 4 July 1999 (Potter and Heilman 2001), leaving significant blow-down timber. Fig. 2*a* shows the temporal variation in simulated HI × TKE_s values at the Ham Lake fire location and estimated incremental fire growth rates during the Ham Lake fire event. Values of HI × TKE_s exceeded 15 $m^2 s^{-2}$ on days 125–127 (5–7 May 2007) and on days 129–131 (9–11 May 2007). Values reached 38.527 $m^2 s^{-2}$ at the fire location at 0400 hours on 7 May 2007 and 25.192 $m^2 s^{-2}$ at 2100 hours on 10 May 2007. Maximum TKE_s values during the 5–7 and 9–11 May 2007 periods reached 7.677 $m^2 s^{-2}$ and 5.038 $m^2 s^{-2}$ respectively. The periods when HI × TKE_s values exceeded 15 $m^2 s^{-2}$ were marked by periods of relatively large increases in burned area. Smaller increases in burned area generally occurred during periods when HI × TKE_s values were less than 15 $m^2 s^{-2}$.

Although observational data for the atmospheric conditions at the Ham Lake fire location are not available for model validation, a comparison of the MM5 simulations of near-surface temperatures and wind speeds with observations at Ely, MN, (available from the US National Climatic Data Center–Global Integrated Surface Hourly Database, http://www.ncdc.noaa.gov, accessed 11 March 2010) suggests that the MM5 simulations captured the overall temporal trends in near-surface temperature and wind speed, at least in the vicinity of the Ham Lake fire (Fig. 2*b*, *c*). The cold bias in MM5-predicted near-surface temperatures (Fig. 2*b*) is consistent with the results of Zhong *et al*. (2005) in their MM5 validation study over the Great Lakes region. However, it is the vertical gradients in temperature and wind speeds that govern the generation of near-surface turbulence, as quantified by TKE_s. Maximum temperatures at Ely, MN, on days 126–127 and 130–131, the same days when there were significant increases in burned area and relative maxima in HI × TKE_s values at the Ham Lake fire location, were

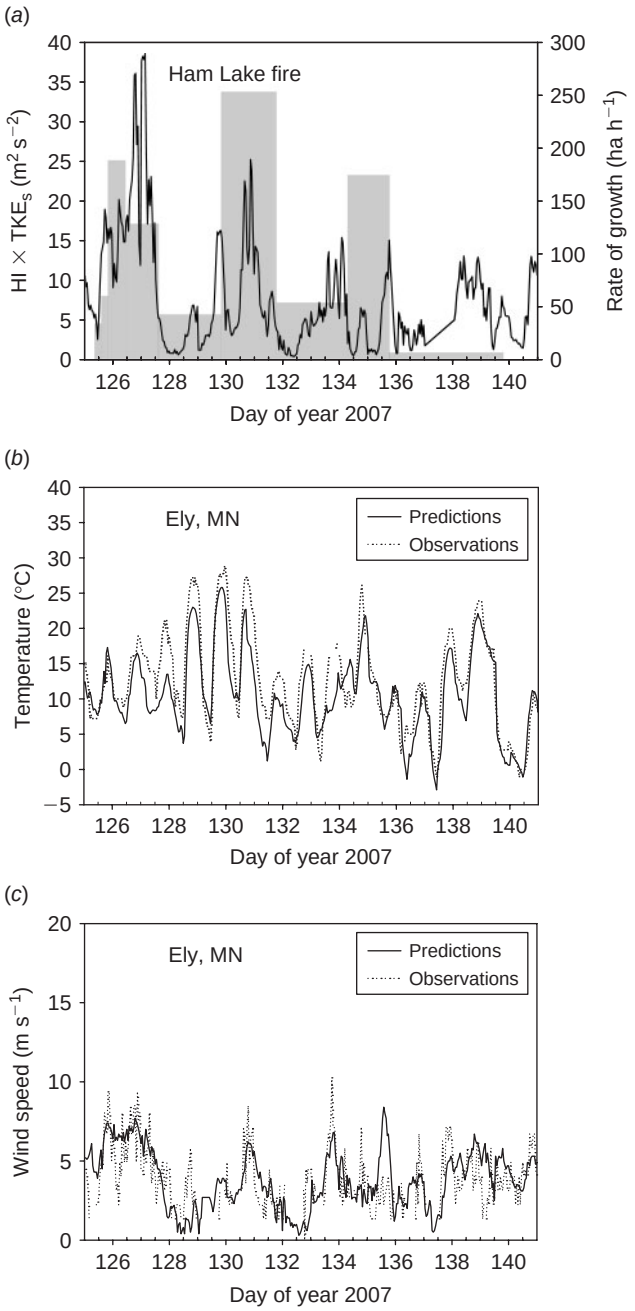

Fig. 2. Time series of (*a*) predicted HI × TKE$_s$ (Haines Index × turbulent kinetic energy at the surface) values and estimated incremental fire growth rates (grey bars) during the Ham Lake, MN, fire from 5 to 20 May 2007 (days 125–140); (*b*) predicted and observed near-surface temperatures at Ely, MN, on days 125–140; and (*c*) predicted and observed near-surface wind speeds at Ely, MN, on days 125–140. The widths of the grey bars in Fig. 2*a* correspond to the time periods over which the fire growth rates were estimated, based on available burn-area reports.

∼17°–18°C and 27°–29°C respectively. Peaks in near-surface wind speeds (8–9 m s^{-1}) at Ely, MN, were also observed on those days (Fig. 2*c*).

Fig. 3 shows the simulated and observed vertical profiles of potential temperature and wind speed at four different times during the Ham Lake fire episode at International Falls, MN, the nearest upper-air radiosonde station to the Ham Lake fire location. Overall, the simulated potential temperature profiles and corresponding vertical gradients compared favourably with the observations (Fig. 3*a*, *b*). The cold bias in the MM5 simulations was confined to levels below 2000 m, with upper levels showing a consistent warm bias. Although differences between simulated and observed wind speed profiles were somewhat more pronounced (Fig. 3*c*, *d*), the wind-speed predictions by MM5 still captured the general patterns in the observed profiles. Only on 13 May 2007 at 1200 hours (day 133) did the MM5 simulation of wind speeds show considerable variation from the observations below 1000 m at the International Falls, MN, site.

Fig. 4 shows the spatial patterns of the HI, TKE$_s$ and HI × TKE$_s$ at 0200 hours on day 127 (7 May 2007) when the Ham Lake fire was undergoing significant growth. This period was marked by a north–south-oriented cold front (primarily a wind-shift boundary) extending through central Minnesota, with relative humidity values less than 50% and southerly to south-easterly winds east of the cold front. Broad areas of HI = 5 (moderate atmospheric potential for extreme fire behaviour) covered Wisconsin, much of Michigan and north-eastern Minnesota where the Ham Lake fire occurred (Fig. 4*a*). Maxima in near-surface atmospheric turbulence were prominent in more isolated areas in north-western Wisconsin, the western upper peninsula of Michigan, south-eastern Minnesota and over the Ham Lake fire location in north-eastern Minnesota (Fig. 4*b*). The HI and TKE$_s$ patterns at 0200 hours on day 127 resulted in an HI × TKE$_s$ pattern shown in Fig. 4*c*. Although the HI pattern at this time suggested a moderate atmospheric potential for extreme fire behaviour in north-eastern Minnesota, extremely high HI × TKE$_s$ values (> 30 m^2 s^{-2}) were present at select locations in the region, including the Ham Lake fire location and along the southern shore of Lake Superior. However, no fires occurred at this time south of Lake Superior.

The second fire case study considered is the Cavity Lake wildfire, which also occurred in the Boundary Waters Canoe Area Wilderness in north-eastern Minnesota (48°6′0.00″N, −91°0′10.80″W). This wildfire started on 14 July 2006 and burned 128.8 km^2 (31 830 acres) until fully contained on 1 September 2006. Fig. 5*a* shows the temporal variation in HI × TKE$_s$ values and the incremental fire growth rates during the first 6 days of the Cavity Lake fire when most of the fire spread occurred. On days 197 (16 July 2006 at 0300 hours), 198 (17 July 2006 at 0200 hours) and 200 (19 July 2006 at 0600 hours), HI × TKE$_s$ values reached 16.138 m^2 s^{-2}, 32.198 m^2 s^{-2} and 19.536 m^2 s^{-2} respectively. The first two occurrences of HI × TKE$_s$ > 15 m^2 s^{-2} during this wildfire event were within a period when the estimated fire growth rate increased from ∼54 to 190 ha h^{-1}. The large fire growth rate (∼483 ha h^{-1}) observed between 2100 hours on day 198 (17 July 2006) and 0300 hours on day 199 (18 July 2006) was not coincident with large HI × TKE$_s$ values. During this 6-h period, HI values were small (2 or 3) while TKE$_s$ values reached a maximum of 2.1 m^2 s^{-2}, a moderately turbulent environment. Observed maximum and minimum near-surface temperatures at Ely, MN, during days 195–200 (14–19 July 2006) were 33.9° and 11.1°C respectively. The MM5 simulations successfully captured the

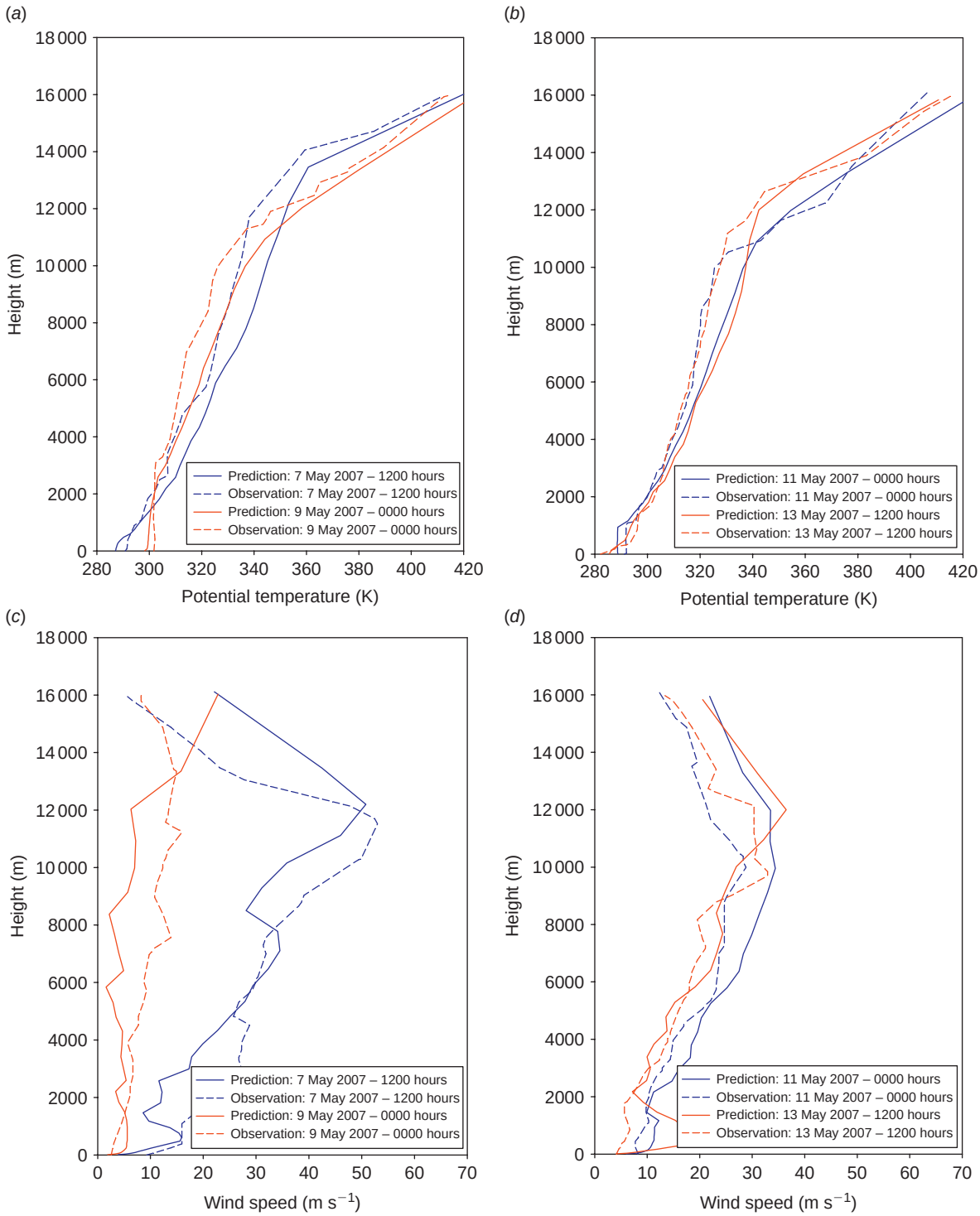

Fig. 3. Predicted and observed vertical profiles of (*a*, *b*) potential temperature, and (*c*, *d*) wind speed at International Falls, MN, on 7 May 2007 (day 127) at 1200 hours; 9 May 2007 (day 129) at 0000 hours; 11 May 2007 (day 131) at 0000 hours; and 13 May 2007 (day 133) at 1200 hours.

diurnal variations and day-to-day trends in temperature at Ely, MN, but generally underpredicted the near-surface temperatures throughout the period (Fig. 5*b*). Predicted wind speeds followed the general trend in observed wind speeds at Ely, MN, which were less than 5 m s^{-1} for much of period except for days 195 and 198 (Fig. 5*c*).

As with the Ham Lake fire episode, the similarity in predicted and observed potential temperature and wind-speed profiles at

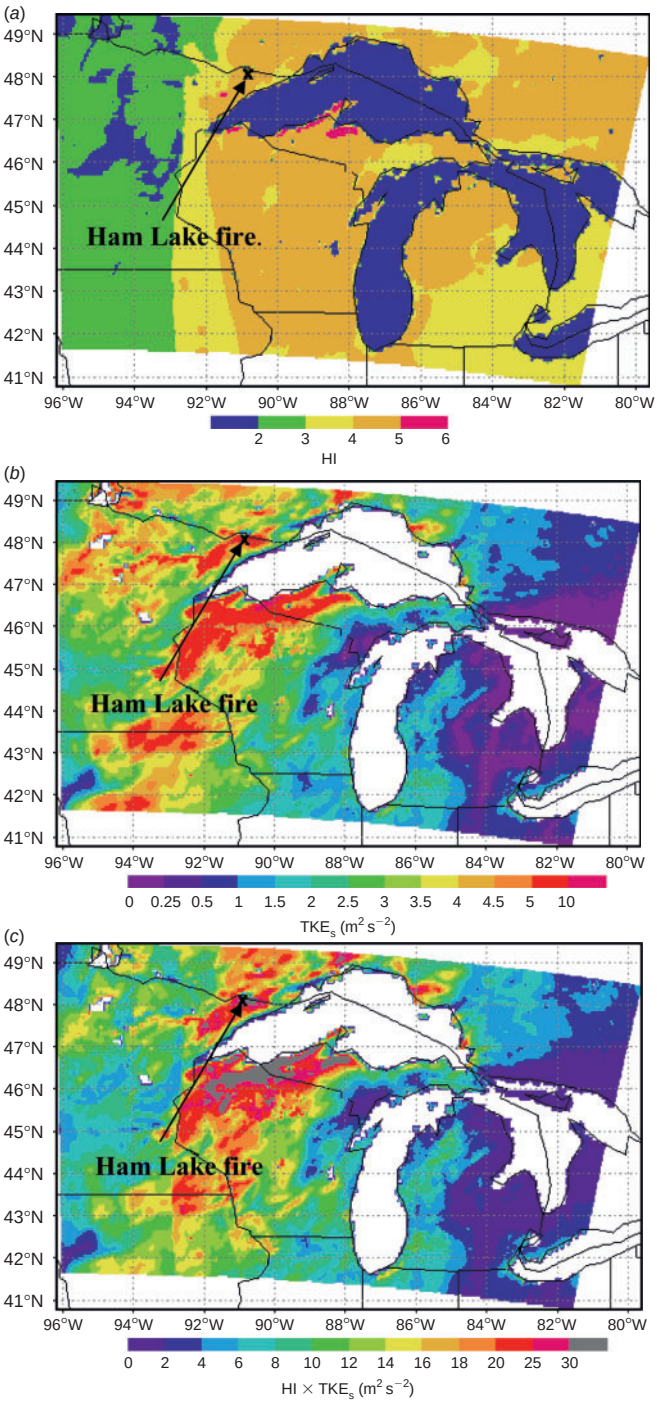

Fig. 4. Simulated spatial patterns of (*a*) HI (Haines Index); (*b*) TKE_s (turbulent kinetic energy at the surface); and (*c*) HI × TKE_s at 0200 hours on 7 May 2007 (day 127) when the Ham Lake, MN, fire was undergoing significant growth. The fire location is indicated by 'x' in each figure.

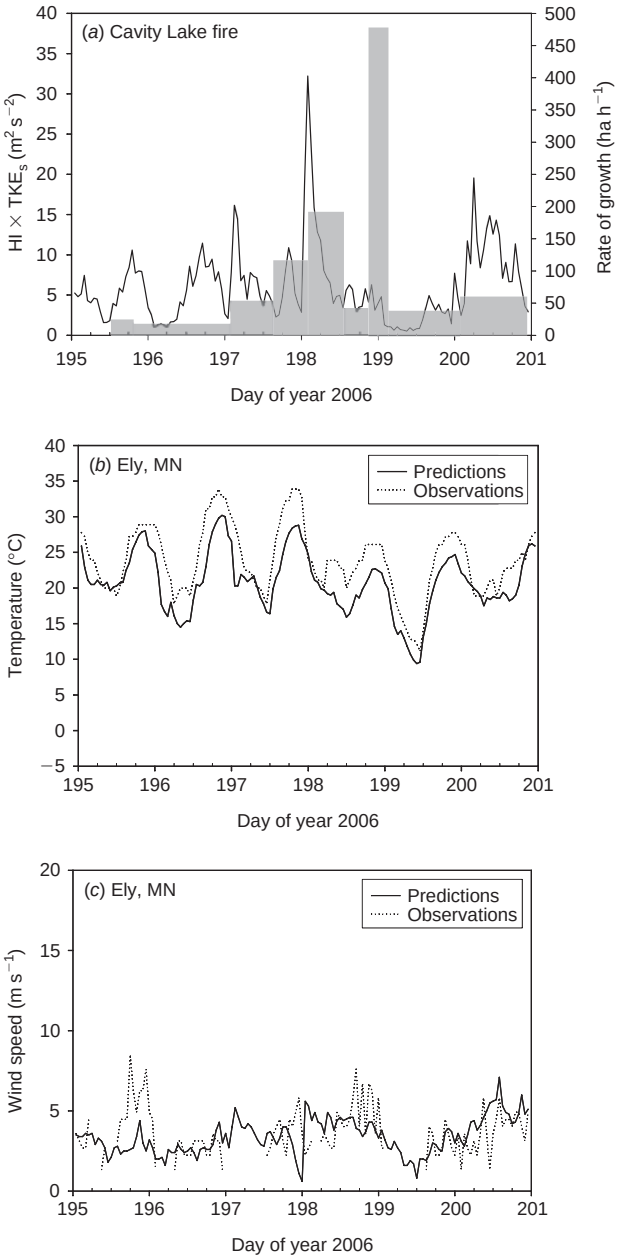

Fig. 5. Time series of (*a*) predicted HI × TKE_s (Haines Index × turbulent kinetic energy at the surface) values and estimated incremental fire growth rates (grey bars) during the Cavity Lake, MN, fire from 14 to 19 July 2006 (days 195–200); (*b*) predicted and observed near-surface temperatures at Ely, MN, on days 195–200; and (*c*) predicted and observed near-surface wind speeds at Ely, MN, on days 195–200. The widths of the grey bars in Fig. 5*a* correspond to the time periods over which the fire growth rates were estimated, based on available burn area reports.

the International Falls, MN, upper air station at a sampling of times (0000 hours and 1200 hours) during the Cavity Lake fire episode suggests that the MM5 was able to capture the overall atmospheric mesoscale conditions prevalent at those times. Fig. 6*a* and *b* reveals predicted and observed potential temperature profiles that were quite similar to each other, especially below 4000 m. The predicted and observed wind-speed profiles at the International Falls, MN, site showed good agreement on days 198 and 199 (17–18 July 2006) at lower and upper levels in the atmosphere (Fig. 6*d*), while on day 197 (16 July 2006), the MM5 overpredicted wind speeds below the 2000 m level.

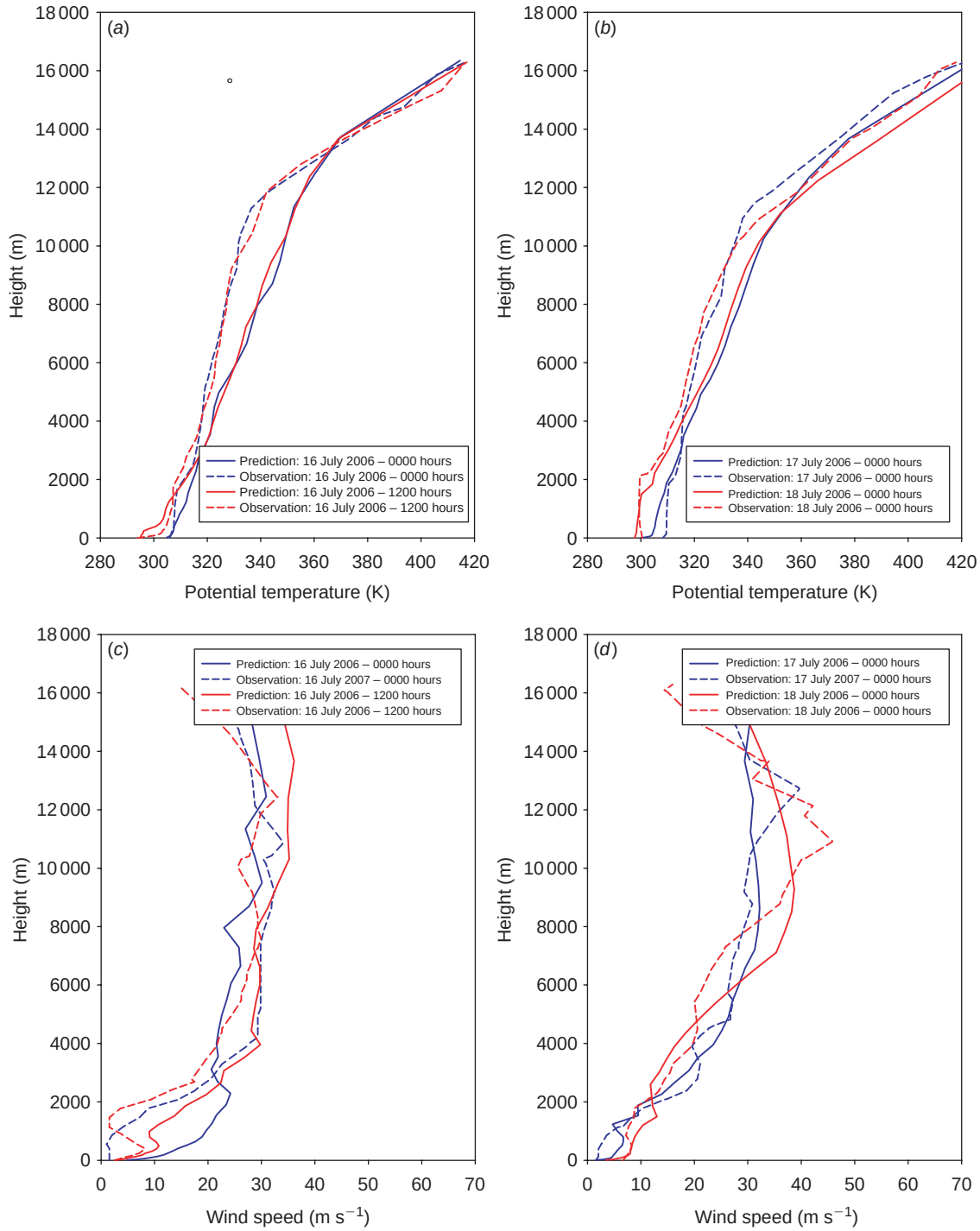

Fig. 6. Predicted and observed vertical profiles of (*a*, *b*) potential temperature; and (*c*, *d*) wind speed at International Falls, MN, on 16 July 2006 (day 197) at 0000 hours; 16 July 2006 (day 197) at 1200 hours; 17 July 2006 (day 198) at 0000 hours; and 18 July 2006 (day 199) at 0000 hours.

The spatial patterns of HI, TKE_s and HI $\times$ TKE_s at 0200 hours on day 198 (17 July 2006) during the Cavity Lake fire are shown in Fig. 7. At this time, a thunderstorm in the vicinity of the Cavity Lake fire generated near-surface winds exceeding 26 m s^{-1}. Haines Index values of 6 (high atmospheric potential for extreme fire behaviour) were common at this time throughout the western Great Lakes region, including the location of the Cavity Lake fire (Fig. 7*a*). However, significant near-surface turbulence was only present in isolated areas of northern Wisconsin, south-western Minnesota and north-eastern Minnesota (Fig. 7*b*). Together, the

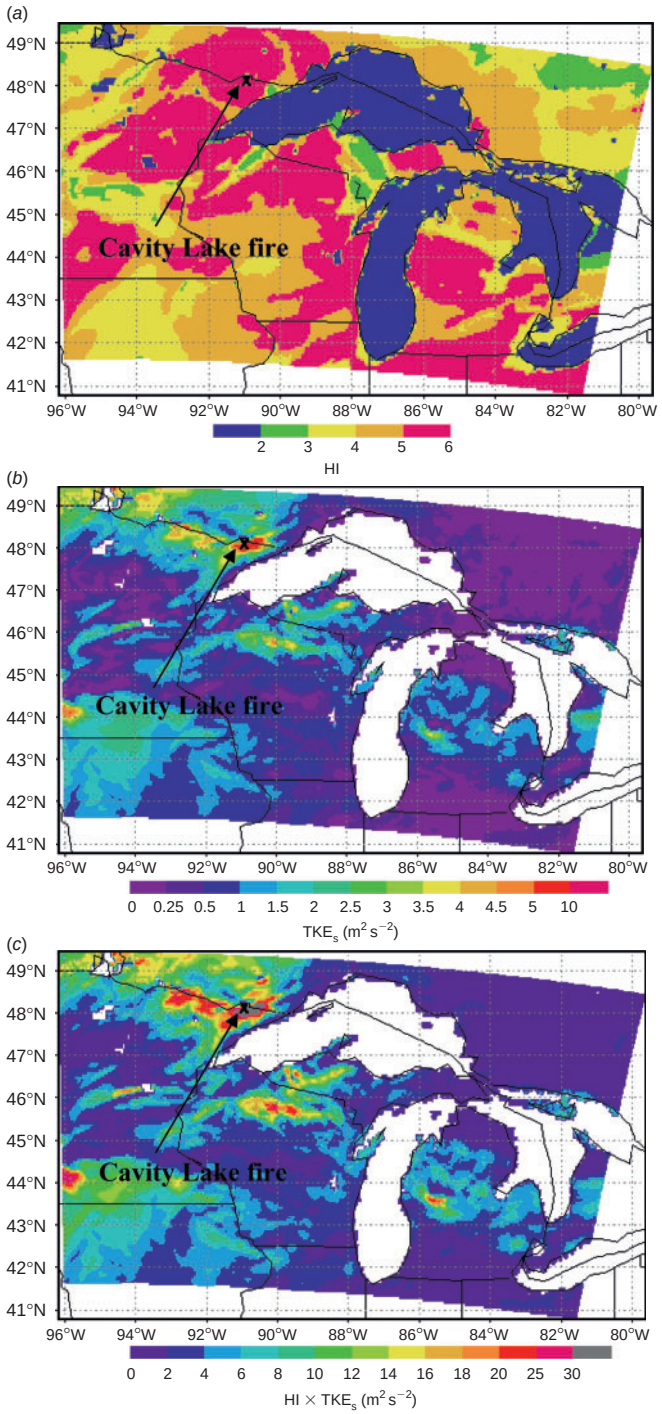

Fig. 7. Simulated spatial patterns of (*a*) HI (Haines Index); (*b*) TKE_s (turbulent kinetic energy at the surface); and (*c*) $HI \times TKE_s$ at 0200 hours on 17 July 2006 (day 198) when the Cavity Lake, MN, fire was undergoing significant growth. The fire location is indicated by 'x' in each figure.

HI and TKE_s patterns produced the $HI \times TKE_s$ pattern at 0200 hours on 17 July 2006 shown in Fig. 7*c*. The largest $HI \times TKE_s$ values ($>30\,m^2\,s^{-2}$) in the western Great Lakes region at this time occurred at the exact location of the Cavity Lake fire, suggesting the atmospheric mesoscale and boundary-layer environments reinforced each other at just the right location and time to significantly impact on the spread of the Cavity Lake fire.

The third wildfire case study considered is the Warren Grove fire that occurred in the Pine Barrens of southern New Jersey near the Atlantic coast (39°42′54.00″N, −74°19′19.20″W). This wildfire started on day 135 (15 May 2007) as the result of a point ignition from a flare dropped from a military aircraft during flight training manoeuvres (US Air Force 2007) and burned 69.9 km^2 (17 270 acres) over a 2-day period. More than 40 km^2 were burned in the initial 3–4 h of the event when $HI \times TKE_s$ values reached 16.831 m^2 s^{-2} (Fig. 8*a*). On day 136 (16 May 2007), $HI \times TKE_s$ values again peaked at 15.589 m^2 s^{-2}, with the cumulative area burned reaching nearly 55 km^2. Fire spread was minimal after day 137 (17 May 2007) during which $HI \times TKE_s$ values were less than 15 m^2 s^{-2}. Predictions of $HI \times TKE_s$ from the MM5 simulations were compared with computed $HI \times TKE_s$ values based on observed near-surface TKE derived from 10-Hz sonic anemometer measurements of wind speeds at a height of 19 m at the nearby USDA Forest Service–New Jersey Weather and Climate Network's Silas Little Experimental Forest flux tower in central New Jersey (http://climate.rutgers.edu/njwxnet, accessed 11 March 2010). The predicted and observed $HI \times TKE_s$ values compared favourably during the period of available observations (15–17 May 2007), although peak values were somewhat underpredicted. Global Integrated Surface Hourly Database observations of near-surface temperatures during this fire event at McGuire Air Force Base, ~35 km north-west of the Warren Grove fire location, indicate temperatures reached a maximum of 27.8° and 30.0°C on days 135 and 136 (Fig. 8*b*). Maximum temperatures on days 137–140 were lower as the result of a synoptic cold front that moved eastward through the Atlantic coastal region. Predicted temperature variability was similar to the observations on days 135–137, including the timing of the passage of the synoptic cold front. As with the previous case studies, the cold bias in the MM5 predictions was prevalent in this case study also. Predicted wind speeds at the McGuire Air Force Base showed good agreement with the observations on days 135–138 when the Warren Grove fire underwent the most rapid spread, but wind speeds were somewhat overpredicted on days 139 and 140 (Fig. 8*c*). Wind speeds on days 135 and 136 reached a maximum of 9.8 m s^{-1} at the McGuire Air Force Base, with lighter winds prevailing on days 137–140.

The nearest upper-air station to the Warren Grove fire location is located in Upton, NY. Comparisons of MM5 predictions of vertical profiles of potential temperature and wind speed with radiosonde observations at Upton, NY, suggest that MM5 was quite successful in simulating the actual thermal and dynamic structure of the atmosphere in the region of and during the Warren Grove fire event (Fig. 9). In particular, the observed strong winds and significant vertical wind shears associated with the low-level jet below the 500-m level on days 135 and 136 (15–16 May 2007) were captured by the MM5 simulations (Fig. 9*c*). These strong vertical wind shears contributed to the generation of near-surface turbulence on days 135 and 136 in the vicinity of the Warren Grove fire.

The HI and TKE_s spatial patterns over the north-eastern US at 1900 hours on day 135 (15 May 2007), approximately 1 h after

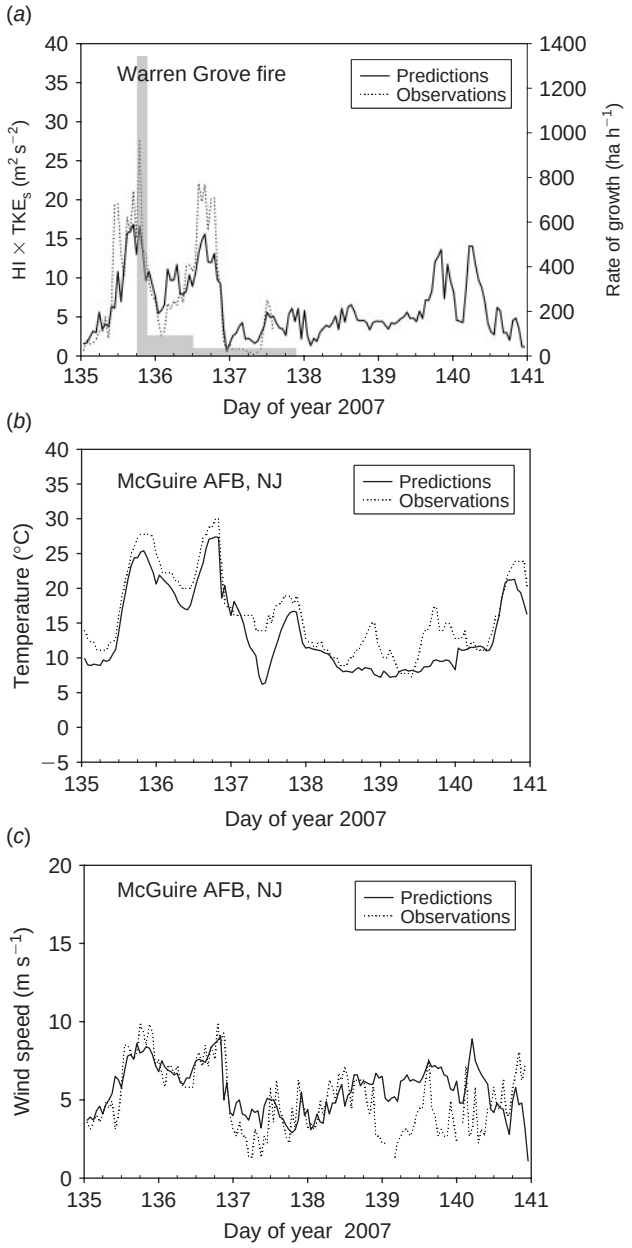

Fig. 8. Time series of (*a*) predicted HI × TKE$_s$ (Haines Index × turbulent kinetic energy at the surface) values and estimated incremental fire growth rates (grey bars) during the Warren Grove, NJ, fire from 15 to 20 May 2007 (days 135–140); (*b*) predicted and observed near-surface temperatures at McGuire Air Force Base, NJ, on days 135–140; and (*c*) predicted and observed near-surface wind speeds at McGuire Air Force Base, NJ, on days 135–140. The widths of the grey bars in Fig. 8*a* correspond to the time periods over which the fire growth rates were estimated, based on available burn area reports. Fig. 8*a* also includes derived HI × TKE$_s$ values from observed near-surface turbulence measurements at the Silas Little Experimental Forest flux tower.

the start of the Warren Grove wildfire (Fig. 10*a*, *b*), indicate lower tropospheric moisture and stability conditions, as quantified by the HI, were most conducive to extreme fire behaviour near the coastal areas in the region and south of Lake Ontario, even though the atmospheric environment throughout the region was highly turbulent (TKE$_s$ > 3 m^2 s^{-2}). Collectively, the HI and TKE$_s$ patterns produced an HI × TKE$_s$ pattern at this time that suggests there was a high potential for extreme and erratic fire behaviour in the same general areas where HI ≥ 5 (Fig. 10*c*). The Warren Grove wildfire in east-central New Jersey was located in one of these areas.

The ambient atmospheric boundary-layer turbulence regimes that developed at the location of and during the large Ham Lake, Cavity Lake and Warren Grove wildfires were primarily the result of buoyancy and shear production of turbulence near the surface. The diffusion or advection of ambient turbulence aloft down to the surface was not a significant factor in creating the highly turbulent ambient conditions near the surface in the vicinity of these wildfires, as shown in the time–height cross-sections in Fig. 11. The turbulence regimes associated with the relative maxima in HI × TKE$_s$ values during the Ham Lake wildfire (days 127, 130–131, 133–134, 135 and 138, as shown in Fig. 2*a*) were all characterised by maximum TKE at or near the surface (Fig. 11*a*). Generally, the presence of any significant turbulence aloft on those days was the result of upward diffusion of turbulence from lower levels. Similarly, the turbulence regimes associated with the relative maxima in HI × TKE$_s$ values during the Cavity Lake (days 197, 198 and 200 in Fig. 5*a*) and Warren Grove (days 135 and 136 in Fig. 8*a*) wildfires were also characterised by maximum TKE at or near the surface (Fig. 11*b*, *c*).

The source of the ambient near-surface turbulence during the Ham Lake, Cavity Lake and Warren Grove wildfires was primarily due to near-surface buoyancy effects. The *Ri* profiles shown in Fig. 12 indicate that buoyancy from the surface up to ~100 m above the surface was the primary mechanism for generating the large TKE in the lower boundary layer when HI × TKE$_s$ values were large during these fires. Above 100 m, thermally neutral and stable conditions prevailed, resulting in *Ri* values greater than 0. Richardson numbers greater than 0.25, indicative of an atmospheric environment where buoyancy completely suppresses any turbulence generated by shear effects, dominated the atmospheric layers above 400–600 m.

Conclusions

We have examined the spatial and temporal patterns of simulated ambient atmospheric boundary-layer TKE during and in the vicinity of major wildfire events (burned area exceeding 0.4047 km^2) that occurred in the western Great Lakes and northeastern US regions over a 29-month period (1 January 2005–31 May 2007). Simulation results from the EAMC's archived MM5-based fire-weather predictions indicate that those wildfire events that burned more than 4.047 km^2 (1000 acres) were more likely to have had occurrences of maximum HI × TKE$_s$ values exceeding 15 m^2 s^{-2}, a threshold indicative of an atmospheric environment highly conducive to extreme and erratic fire behaviour, than for those wildfire events that burned less than 4.047 km^2. The corresponding difference in mean TKE$_s$ values at the time of maximum HI × TKE$_s$ for the two groups of wildfire events was statistically significant whereas the difference in median HI values at the time of maximum HI × TKE$_s$ was not statistically significant. These results suggest that, at least for

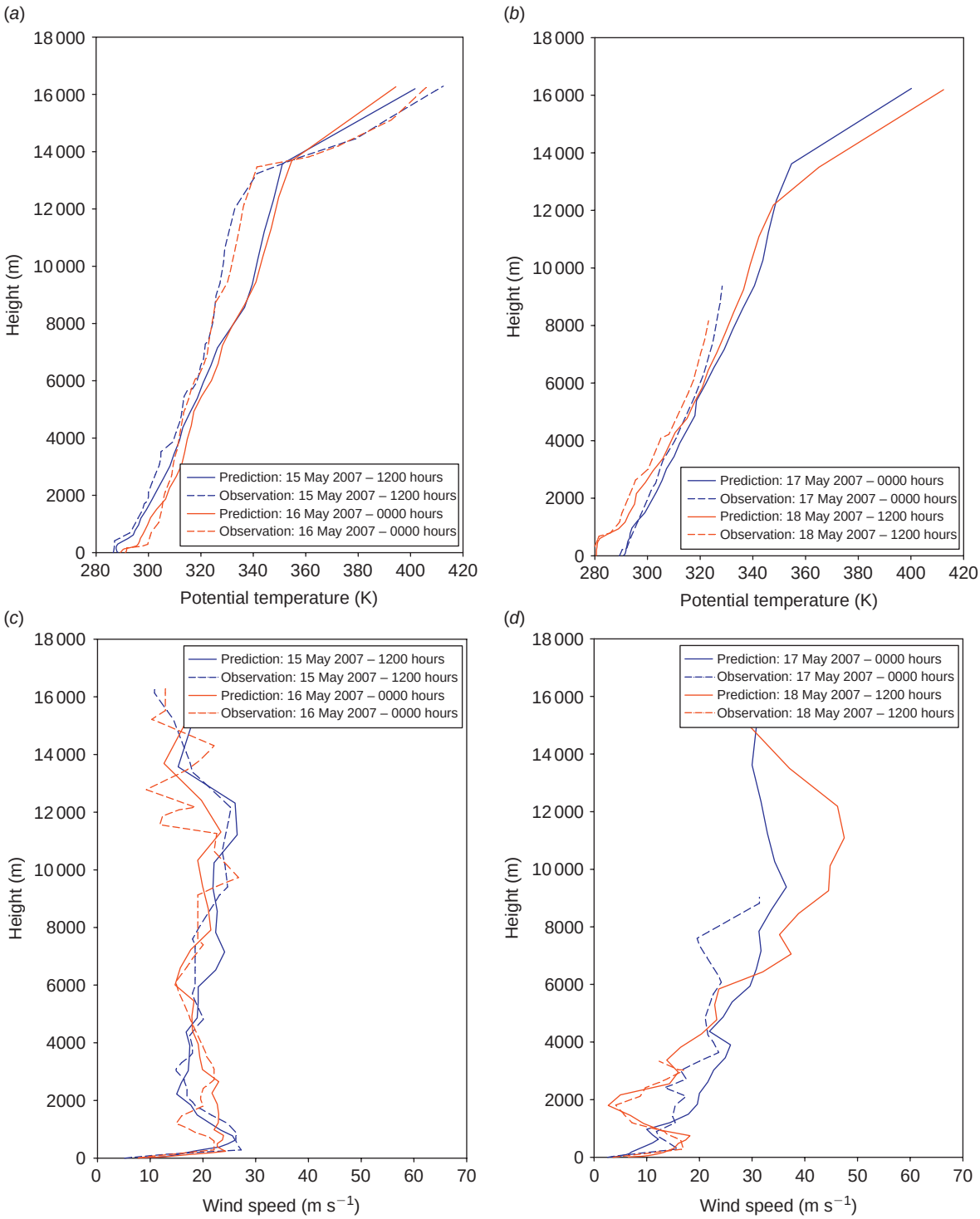

Fig. 9. Predicted and observed vertical profiles of (*a*, *b*) potential temperature, and (*c*, *d*) wind speed at Upton, NY, on 15 May 2007 (day 135) at 1200 hours; 16 May 2007 (day 136) at 0000 hours; 17 May 2007 (day 137) at 0000 hours; and 18 May 2007 (day 138) at 1200 hours.

wildfire events in the western Great Lakes and north-eastern US regions, a near-surface turbulence-based fire-weather index may be a better discriminating atmospheric indicator of the potential for extreme and erratic fire behaviour than the HI.

The duration of individual episodes of TKE_s exceeding $3\ m^2\ s^{-2}$ (a highly turbulent environment) during the large wildfire events considered in this study was highly variable. Some episodes of TKE_s values exceeding the $3\text{-}m^2\ s^{-2}$ threshold lasted

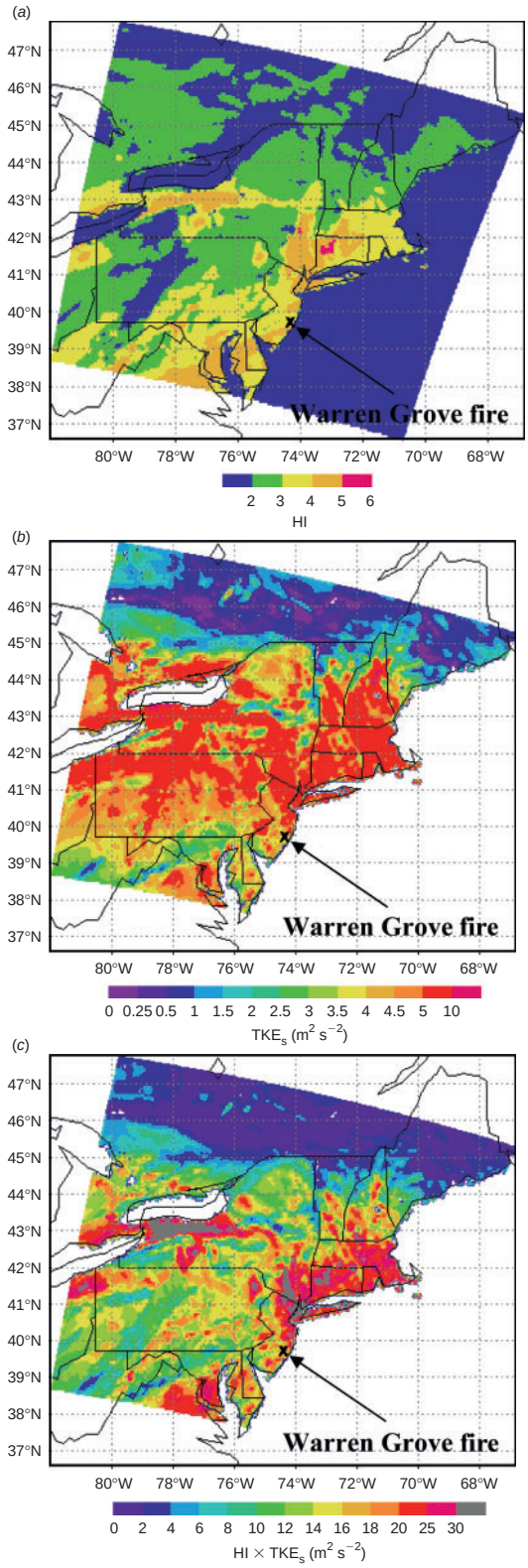

Fig. 10. Simulated spatial patterns of (*a*) HI (Haines Index); (*b*) TKE_s (turbulent kinetic energy at the surface); and (*c*) $HI \times TKE_s$ at 1900 hours on 15 May 2007 (day 135) when the Warren Grove, NJ, fire was undergoing significant growth. The fire location is indicated by 'x' in each figure.

for multiple hours (e.g. 49 h during the Ham Lake fire), although many episodes were as short as 1 h. Previous model-based analyses (Heilman and Bian 2007) of TKE_s values over the western Great Lakes region at 2000 hours UTC (local mid-afternoon) for all days in 2006 suggest that exceedances of the 3-$m^2\,s^{-2}$ threshold at any location are a fairly rare event (approximately once every 10 days). However, a true comparison of the frequencies and durations of occurrence of high TKE_s and high $HI \times TKE_s$ episodes during wildfire events with the expected or typical frequencies and durations at fire locations requires a long-term analysis of the climatological patterns of turbulence regimes over the region. The recent release of the North American Regional Reanalysis (NARR) dataset (Mesinger *et al*. 2006), an atmospheric and land surface hydrology dataset at 32-km resolution, which covers the 1979-present period and includes TKE and temperature and dew point temperature data for computing the HI, provides an excellent opportunity for examining the spatial and temporal patterns of TKE_s and $HI \times TKE_s$ over different regions of North America. As a follow-up to the present study, a NARR-based climatological analysis of lower atmospheric TKE and associated $HI \times TKE_s$ patterns and trends over the US has been initiated to provide baseline-frequency climatologies for comparisons with ambient turbulence variability during actual large and small wildfire events.

The generation of ambient near-surface turbulence during the wildfire events included in this study was primarily buoyancy-driven. A Richardson number analysis showed that near-surface buoyancy at the time of maximum $HI \times TKE_s$ dominated mechanical wind shear effects in creating the ambient boundary-layer turbulence regimes that interacted with the wildfires, although those wildfire events that burned more than 4.047 km^2 were more often associated with larger ambient wind shears than wildfires that burned less area.

Case studies of the three largest wildfires to occur during the 1 January 2005–31 May 2007 period in the western Great Lakes and north-eastern US regions showed that the periods of highest fire growth tended to coincide with periods when $HI \times TKE_s$ values exceeded 15 $m^2\,s^{-2}$. Vertical profiles of ambient TKE during these wildfire events indicate that the boundary-layer turbulence regimes were characterised by maximum turbulence at or near the surface when $HI \times TKE_s$ values were large. The downward transport of turbulence from higher levels in the atmosphere via advection or diffusion was not a significant factor in contributing to the significant ambient near-surface turbulence in the vicinity of the wildfires. When $HI \times TKE_s$ values were large, buoyancy primarily contributed to the generation of turbulence in the boundary layer up to ~100 m above the surface. Wind-shear effects dominated from ~100–600 m above the surface, above which buoyancy tended to dissipate any turbulence generated by wind-shear effects.

A limiting factor encountered in this study of ambient atmospheric turbulence environments in the vicinity of wildfires was the lack of high-frequency fire growth data for comparison with simulated TKE variability during fire events. The length and time scales of turbulent eddies that make the most contributions to TKE in the atmospheric boundary layer are on the order of 10 to 100 m and 10 s to 10 min respectively (Stull 1988). Accordingly, the interactions of these ambient turbulent eddies with wildfires and the associated turbulence regimes generated by the fires will

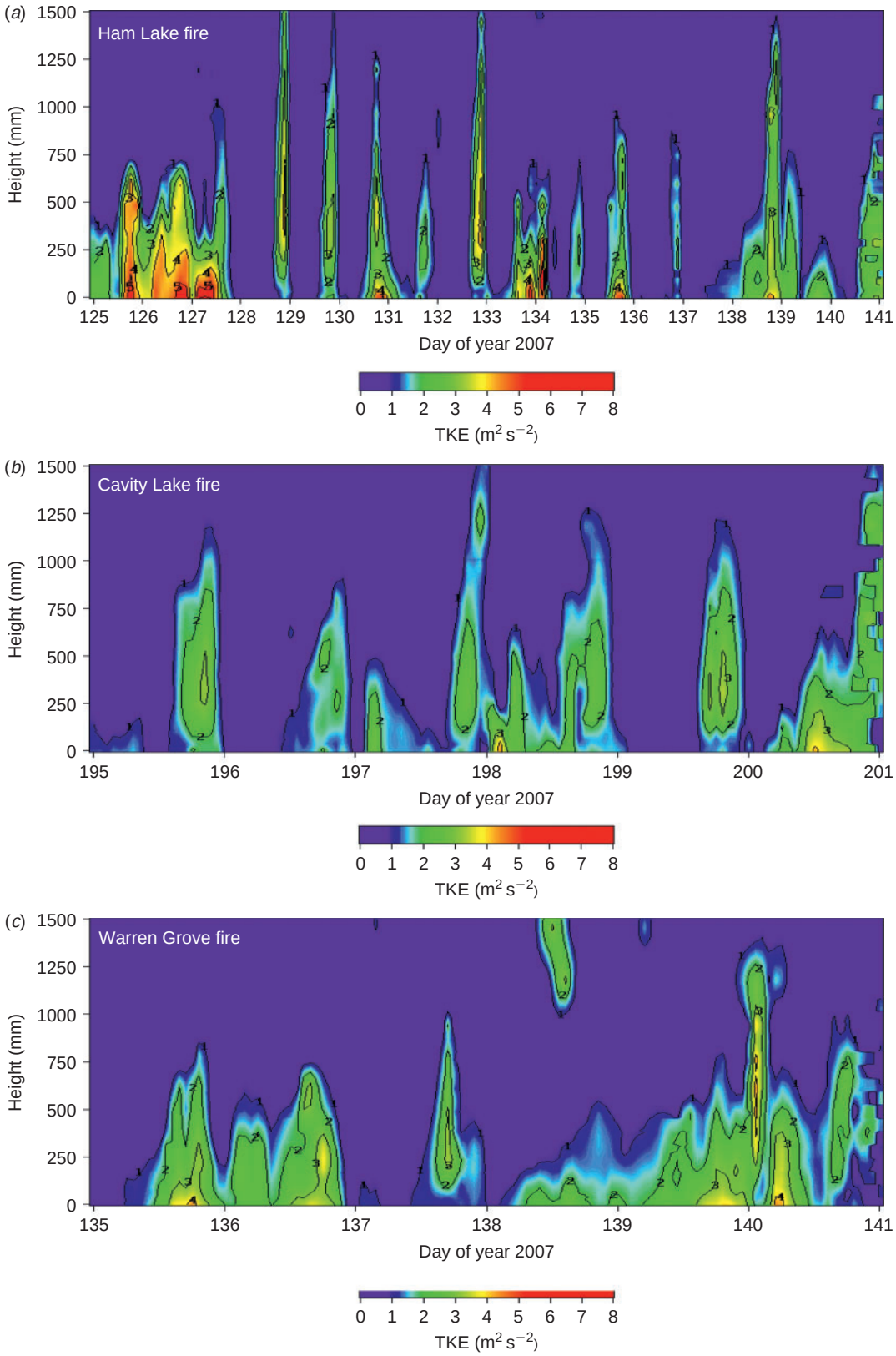

Fig. 11. Simulated time-height cross-sections of TKE (turbulent kinetic energy) during the (*a*) Ham Lake, MN; (*b*) Cavity Lake, MN; and (*c*) Warren Grove, NJ, wildfires.

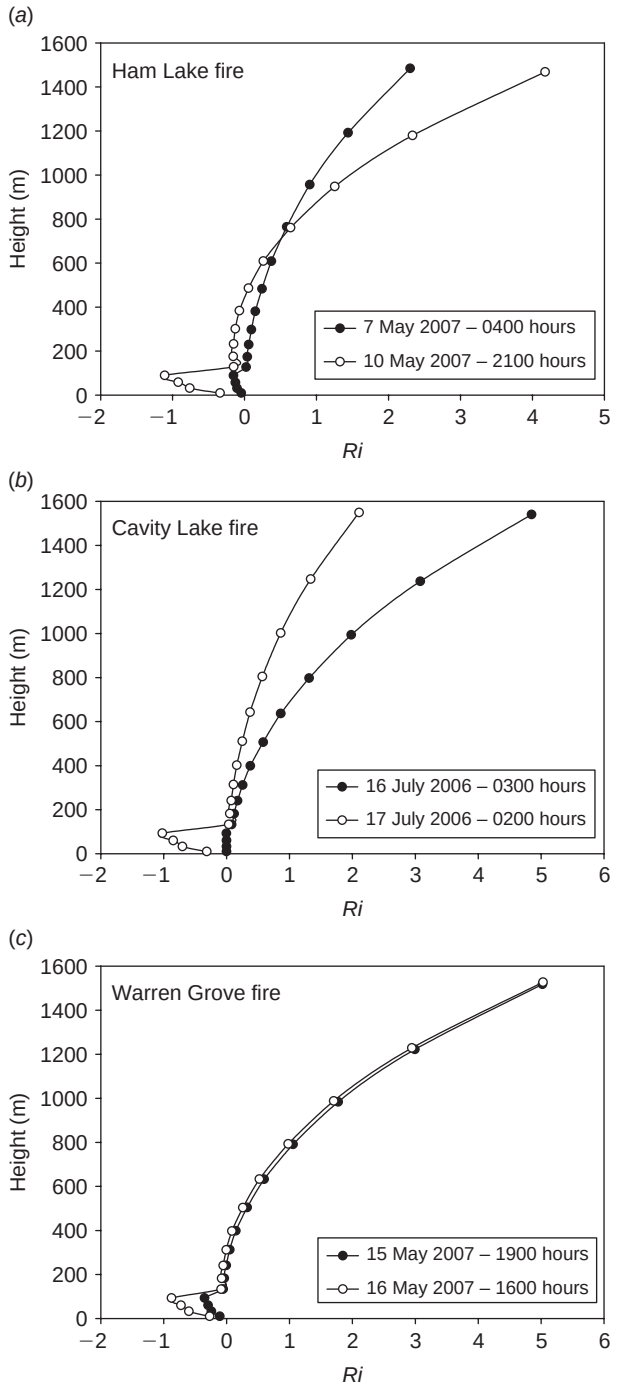

Fig. 12. Vertical profiles of the *Ri* (Richardson number) at two periods when values of the HI × TKE_s (Haines Index × turbulent kinetic energy at the surface) were large during the (*a*) Ham Lake, MN; (*b*) Cavity Lake, MN; and (*c*) Warren Grove, NJ, wildfires.

occur at similar spatial and temporal scales. Thus, measurements of fire growth that can be used to assess the potential response of fires to ambient atmospheric turbulence regimes should ideally be made at spatial and temporal resolutions similar to the size and duration of the turbulent eddies that characterise the atmospheric boundary layer. Although that level of fire-growth monitoring is rare during actual wildfires, the recent and ongoing emphasis of *in situ* monitoring of fire–fuel–atmosphere interactions within experimental burns (e.g. FireFlux experiment, Clements *et al*. 2007, 2008; Rx-CADRE experiment, O'Brien 2008) will provide much-needed high-frequency fire growth and turbulence data for assessing the relationship between near-surface ambient turbulence and the occurrence of erratic and extreme fire behaviour.

The analyses described here represent a first step in assessing the association of significant atmospheric boundary layer turbulence with extreme and erratic fire behaviour and the feasibility of using TKE either alone or in combination with other indices like the HI as an indicator of how conducive the atmosphere may be to erratic fire spread. With the availability of turbulence predictions from many current high-resolution operational and research-based atmospheric mesoscale and boundary-layer models, it is now possible to incorporate turbulence-related variables like TKE into fire-weather assessments. This study suggests that model predictions of TKE and the underlying physical processes involved in generating boundary-layer turbulence regimes may provide additional tools for characterising the atmospheric potential for dangerous fire conditions, at least in the western Great Lakes and north-eastern US regions. Additional analyses of turbulence behaviour during wildfire events in other regions of the US and elsewhere are needed to assess the efficacy of boundary-layer turbulence predictions for fire-weather assessments in other geographic areas.

Acknowledgements

The authors thank Dr Kenneth Clark, USDA Forest Service, for providing observational turbulence data collected at the Silas Little Experimental Forest in New Jersey. Funding for this research was provided by the US National Fire Plan.

References

Byun D, Schere KL (2006) Review of the governing equations, computational algorithms, and other components of the Models-3 Community Multiscale Air Quality (CMAQ) Modeling System. *Applied Mechanics Reviews* **59**, 51–77. doi:10.1115/1.2128636

Chien F-C, Kuo YH, Yang M-J (2002) Preciptation forecast of MM5 in the Taiwan area during the 1998 Mei-yu season. *Weather and Forecasting* **17**, 739–754. doi:10.1175/1520-0434(2002)017<0739:PFOMIT>2.0.CO;2

Clark TL, Radke L, Coen J, Middleton D (1999) Analysis of small-scale convective dynamics in a crown fire using infrared video camera imagery. *Journal of Applied Meteorology* **38**, 1401–1420. doi:10.1175/1520-0450(1999)038<1401:AOSSCD>2.0.CO;2

Clark TL, Coen J, Latham D (2004) Description of a coupled atmosphere–fire model. *International Journal of Wildland Fire* **13**, 49–63. doi:10.1071/WF03043

Clements CB, Potter BE, Zhong S (2006) *In situ* measurements of water vapor, heat, and CO_2 fluxes within a prescribed grass fire. *International Journal of Wildland Fire* **15**, 299–306. doi:10.1071/WF05101

Clements CB, Zhong S, Goodrick S, Li J, Potter BE, Bian X, Heilman WE, Charney JJ, *et al.* (2007) Observing the dynamics of wildland grass fires: FireFlux – a field validation experiment. *Bulletin of the American Meteorological Society* **88**, 1369–1382. doi:10.1175/BAMS-88-9-1369

Clements CB, Zhong S, Bian X, Heilman WE, Byun DW (2008) First observations of turbulence generated by grass fires. *Journal of Geophysical Research* **113**, D22102. doi:10.1029/2008JD010014

Coen JL (2005) Simulation of the Big Elk Fire using coupled atmosphere–fire modeling. *International Journal of Wildland Fire* **14**, 49–59. doi:10.1071/WF04047

Coen J, Mahalingam S, Daily J (2004) Infrared imagery of crown-fire dynamics during FROSTFIRE. *Journal of Applied Meteorology* **43**, 1241–1259. doi:10.1175/1520-0450(2004)043<1241:IIOCDD>2.0.CO;2

Colle B, Westrick KJ, Mass C (1999) Evaluation of MM5 and Eta-10 precipitation forecasts over the Pacific North-west during the cool season. *Weather and Forecasting* **14**, 137–154. doi:10.1175/1520-0434(1999)014<0137:EOMAEP>2.0.CO;2

Colle B, Mass CF, Westrick KJ (2000) MM5 precipitation verification over the Pacific North-west during the 1997–99 seasons. *Weather and Forecasting* **15**, 730–744. doi:10.1175/1520-0434(2000)015<0730:MPVOTP>2.0.CO;2

Colle B, Olson JB, Tongue JS (2003*a*) Multiseason verification of the MM5. Part I: Comparison with the Eta model over the central and eastern United States and impact of MM5 resolution. *Weather and Forecasting* **18**, 431–457. doi:10.1175/1520-0434(2003)18<431:MVOTMP>2.0.CO;2

Colle B, Olson JB, Tongue JS (2003*b*) Multiseason verification of the MM5. Part II: Evaluation of high-resolution precipitation forecasts over the north-eastern United States. *Weather and Forecasting* **18**, 458–480. doi:10.1175/1520-0434(2003)18<458:MVOTMP>2.0.CO;2

Cunningham P, Goodrick SL, Hussaini MY, Linn RR (2005) Coherent vortical structures in numerical simulations of buoyant plumes from wildland fires. *International Journal of Wildland Fire* **14**, 61–75. doi:10.1071/WF04044

de Arellano JVG, Vellinga OS, Holtlag AAM, Bosveld FC, Baltink HK (2001) Observational evaluation of PBL parameterizations modeled by MM5. In 'Proceedings of the 11th PSU/NCAR Mesoscale Model User's Workshop', 25–27 June 2001, Boulder, CO. pp. 102–104. (National Center for Atmospheric Research: Boulder, CO)

Ferguson SA, McKay S, Nagel D, Piepho T, Rorig M, Anderson C (2001) The potential for smoke to ventilate from wildland fires in the United States. In 'Fourth Symposium on Fire and Forest Meteorology', 12–15 November 2001, Reno, NV. (American Meteorological Society: Boston, MA) Available at http://ams.confex.com/ams/4FIRE/techprogram/meeting_4FIRE.htm [Verified 13 March 2010]

Fosberg MA (1978) Weather in wildland fire management: the fire weather index. In 'Proceedings of the Conference on Sierra Nevada Meteorology', 19–21 June 1978, Lake Tahoe, CA. pp. 1–4. (American Meteorological Society: Boston, MA)

Gerrity JP, Black TL, Treadon RE (1994) The numerical solution of the Mellor-Yamada level 2.5 turbulent kinetic energy equation in the Eta model. *Monthly Weather Review* **122**, 1640–1646. doi:10.1175/1520-0493(1994)122<1640:TNSOTM>2.0.CO;2

Grell GA, Dudhia J, Stauffer DR (1994) A description of the fifth-generation Penn State/NCAR mesoscale model (MM5). National Center for Atmospheric Research, NCAR Technical Note NCAR/TN-398+STR. (Boulder, CO)

Haines DA (1988) A lower atmospheric severity index for wildland fires. *National Weather Digest* **13**, 23–27.

Heilman WE (1994) Simulations of buoyancy-generated horizontal roll vortices over multiple heating lines. *Forest Science* **40**, 601–617.

Heilman WE, Bian X (2007) Combining turbulent kinetic energy and Haines Index predictions for fire-weather assessments. In 'Proceedings of the 2nd Fire Behavior and Fuels Conference', 26–30 March 2007, Destin, FL. (Eds BW Butler, W Cook) USDA Forest Service, Rocky Mountain Research Station, Proceedings RMRS-P-46CD, pp. 159–172. (Fort Collins, CO)

Jenkins MA (2002) An examination of the sensitivity of numerically simulated wildfires to low-level atmospheric stability and moisture, and the consequences for the Haines Index. *International Journal of Wildland Fire* **11**, 213–232. doi:10.1071/WF02006

Linn RR, Cunningham P (2005) Numerical simulations of grass fires using a coupled atmosphere–fire model: basic fire behavior and dependence on wind speed. *Journal of Geophysical Research* **110**, D13107. doi:10.1029/2004JD005597

Linn R, Reisner J, Colman JJ, Winterkamp J (2002) Studying wildfire behavior using FIRETEC. *International Journal of Wildland Fire* **11**, 233–246. doi:10.1071/WF02007

Linn R, Winterkamp J, Colman JJ, Edminster C, Bailey JD (2005) Modeling interactions between fire and atmosphere in discrete fuel beds. *International Journal of Wildland Fire* **14**, 37–48. doi:10.1071/WF04043

Linn R, Winterkamp J, Edminster C, Colman JJ, Smith WS (2007) Coupled influences of topography and wind on wildland fire behavior. *International Journal of Wildland Fire* **16**, 183–195. doi:10.1071/WF06078

Manning KW, Davis CA (1997) Verification and sensitivity experiments for the WISP94 MM5 forecasts. *Weather and Forecasting* **12**, 719–735. doi:10.1175/1520-0434(1997)012<0719:VASEFT>2.0.CO;2

Mell W, Jenkins MA, Gould J, Cheney P (2007) A physics-based approach to modeling grassland fires. *International Journal of Wildland Fire* **16**, 1–22. doi:10.1071/WF06002

Mellor GL, Yamada T (1974) A hierarchy of turbulence closure models for planetary boundary layers. *Journal of the Atmospheric Sciences* **31**, 1791–1806. doi:10.1175/1520-0469(1974)031<1791:AHOTCM>2.0.CO;2

Mellor GL, Yamada T (1982) Development of a turbulence closure model for geophysical fluid problems. *Reviews of Geophysics and Space Physics* **20**, 851–875. doi:10.1029/RG020I004P00851

Mesinger F, DeMego G, Kalnay E, Mitchell K, Shafran PC, Ebisuzaki W, Jović D, Woollen J, *et al.* (2006) North American regional reanalysis. *Bulletin of the American Meteorological Society* **87**, 343–360. doi:10.1175/BAMS-87-3-343

O'Brien JJ (2008) Collaborative research in the core fire sciences: prescribed fire combustion–atmospheric dynamics research experiments (Rx-CADRE). *Southern Smoke Issues* **1**, 7–10.

Potter BE, Heilman WE (2001) Atmospheric research needs and issues. In 'Northern Minnesota Independence Day Storm: a Research Needs Assessment'. (Eds WJ Mattson, DS Shriner) USDA Forest Service, North Central Research Station, General Technical Report NC-216, pp. 9–11. (Saint Paul, MN)

Reisner J, Rasmussen RJ, Bruintjes RT (1998) Explicit forecasting of supercooled liquid water in winter storms using the MM5 mesoscale model. *Quarterly Journal of the Royal Meteorological Society* **124**, 1071–1107. doi:10.1002/QJ.49712454804

Stull RB (1988) 'An Introduction to Boundary Layer Meteorology.' (Kluwer Academic Publishers: Dordrecht, the Netherlands)

Sun R, Krueger SK, Zulauf MA, Jenkins MA, Charney JJ (2006) Wildfire evolution in the convective boundary layer. In 'Proceedings of the 17th Symposium on Boundary Layers and Turbulence', 21–25 May 2006, San Diego, CA. (American Meteorological Society: Boston, MA)

US Air Force (2007) United States Air Force Aircraft Accident Investigation Board Report. (New Jersey Air National Guard: Atlantic City International Airport, NJ)

USDA Forest Service (2002) National Fire Plan research and development – 2001 business summary. USDA Forest Service, North Central Research Station. (Saint Paul, MN)

Zhong S, Fast J (2003) An evaluation of the MM5, RAMS, and Meso-Eta models at subkilometer resolution using VTMX field campaign data in the Salt Lake Valley. *Monthly Weather Review* **131**, 1301–1322. doi:10.1175/1520-0493(2003)131<1301:AEOTMR>2.0.CO;2

Zhong S, In H-J, Bian X, Charney J, Heilman W, Potter B (2005) Evaluation of real-time high-resolution MM5 predictions over the Great Lakes region. *Weather and Forecasting* **20**, 63–81. doi:10.1175/WAF-834.1

Manuscript received 17 May 2008, accepted 30 July 2009